Final Project Report

PLASMA-ASSISTED CATALYTIC REDUCTION OF NOx FROM STATIONARY DIESEL ENGINES

SERDP Project CP-1077

Bernie M. Penetrante and Raymond C. Brusasco
Lawrence Livermore National Laboratory
Livermore, California

And

Joseph D. Wander
Air Force Research Laboratory
Tyndall AFB, Florida

Submitted 15 July 2001

Report Documentation Page

Form Approved
OMB No. 0704-0188

1. REPORT DATE	2. REPORT TYPE	3. DATES COVERED
JUL 2001		**00-00-2001 to 00-00-2001**

4. TITLE AND SUBTITLE	5a. CONTRACT NUMBER
Plasma-Assisted Catalytic Reduction of NOx from Stationary Diesel Engines	5b. GRANT NUMBER
	5c. PROGRAM ELEMENT NUMBER
6. AUTHOR(S)	5d. PROJECT NUMBER
	5e. TASK NUMBER
	5f. WORK UNIT NUMBER
7. PERFORMING ORGANIZATION NAME(S) AND ADDRESS(ES) **Lawrence Livermore National Laboratory,7000 East Ave,Livermore,CA,94550-9234**	8. PERFORMING ORGANIZATION REPORT NUMBER
9. SPONSORING/MONITORING AGENCY NAME(S) AND ADDRESS(ES)	10. SPONSOR/MONITOR'S ACRONYM(S)
	11. SPONSOR/MONITOR'S REPORT NUMBER(S)

12. DISTRIBUTION/AVAILABILITY STATEMENT
Approved for public release; distribution unlimited

13. SUPPLEMENTARY NOTES

14. ABSTRACT

15. SUBJECT TERMS

16. SECURITY CLASSIFICATION OF:			17. LIMITATION OF ABSTRACT	18. NUMBER OF PAGES	19a. NAME OF RESPONSIBLE PERSON
a. REPORT **unclassified**	b. ABSTRACT **unclassified**	c. THIS PAGE **unclassified**	**Same as Report (SAR)**	**55**	

Introduction

Diesel engines are widely used throughout the Department of Defense (DoD) for powering tactical and non-tactical vehicles and vessels, off-road equipment, engine-generator sets, aircraft ground-support equipment, and a variety of other applications. Current and proposed air pollution regulations are expected to impact the use of these diesel engines. Current catalyst technology is capable of reducing particulates, carbon monoxide and hydrocarbons (HCs). No satisfactory solution currently exists for nitrogen oxides (NOx). For more than a decade, investigators have been searching for suitable catalysts that can selectively reduce NOx in the presence of a reductant. The process is known as selective catalytic reduction (SCR). Such a technology, using ammonia as a reductant, does exist. However, the use of hydrocarbons such as diesel fuel or jet propulsion fuel as a reductant is a more feasible, cost-effective, and environmentally sound approach, particularly for mobile applications. The search for effective and durable SCR catalysts that work with HCs (also known as lean-NOx catalysts) in diesel exhaust environments is a high-priority issue in emissions control and the subject of intense investigations by engine and catalyst companies, and universities, throughout the world. More than 50 lean-NOx catalysts have been reported in the research and patent literature. However, important unresolved technical and economic problems have plagued these catalysts and prevented their widespread application. An approach for resolving the most important of these problems—catalyst durability in the presence of soot, fuel sulfur and high-temperature water vapor—has been developed by Lawrence Livermore National Laboratory in collaboration with Cummins Engine Company and Engelhard Corporation. The process is known as Plasma-Assisted Catalytic Reduction (PACR). In this SERDP project, the Air Force Research Laboratory and Lawrence Livermore National Laboratory team conducted feasibility testing of the PACR process using laboratory, pilot-scale and full-scale prototypes.

The goal of this project was to devise methods to allow military mobile power generators, in particular aerospace ground equipment (AGE), to meet air pollution control targets set by state and local environmental regulations, while addressing issues associated with maintainability and operability of the military fleet. For diesel-powered AGE, this means a control strategy that concerns itself with soot and NOx emissions.

Technical Description

Diesel engines operate under lean-burn (high air-to-fuel ratio) conditions. The amount of oxygen in the exhaust stream of diesel engines is around 10 percent, much higher than that from gasoline engines. The high oxygen content makes the three-way catalytic converter of today's gasoline automobiles unsuitable for NOx removal in diesel engine exhaust. The excess oxygen adsorbs preferentially on the precious metal (Pt, Rh, and Pd) surfaces in the catalyst, thus inhibiting the chemical reduction of NOx to N_2.
There are currently no known catalysts that can decompose NOx to N_2 and O_2 in oxygen-rich environments. The only fallback is to use catalysts that can selectively reduce NOx

in the presence of a reductant. Such a technology, using ammonia as a reductant, does exist. However, ammonia is both a hazardous material and an extra logistical element.

Catalysts that selectively promote reduction of NOx under oxygen-rich conditions, in the presence of HCs, are known as lean-NOx catalysts. More than 50 such catalysts have been reported in the literature. Unfortunately, the known lean-NOx catalysts are hydrothermally unstable and/or easily poisoned by fuel sulfur, resulting in noticeable loss of activity after only a short operation time. Much effort has been devoted to improving the activity and durability of these catalysts, but the results are still far from satisfactory.

Empirical evidence is accumulating suggesting that NOx reduction by lean-NOx catalysts proceeds by first converting the NO into NO_2 either in the gas phase or on the surface. The NO_2 is then reduced on the catalyst surface in the presence of HCs. The deactivation of catalyst activity by water vapor may be related to the deactivation of sites responsible for NO oxidation. Once the NO oxidation sites are deactivated, the catalyst loses competitiveness for HC reduction of NOx versus HC combustion by oxygen, thereby leading to inefficient NOx removal.

Oxidizing NO to $NO2_2$ in the plasma allows the function of the catalyst to be devoted exclusively to the selective reduction of NO_2 by the HCs. In the plasma, the HC serves to enhance the oxidation of NO to NO_2. In the catalyst, the HC serves to reduce NO_2 to N_2. The process, known as plasma-assisted catalytic reduction (PACR), may be expressed schematically in two steps:

$$\text{plasma} + NO + O_2 + HC \rightarrow NO_2 + \text{HC breakup products}$$
$$\text{catalyst} + NO_2 + HC \rightarrow N_2 + CO_2 + H_2O$$

where HC refers to hydrocarbon molecules. Figure 1 depicts a schematic of the system.

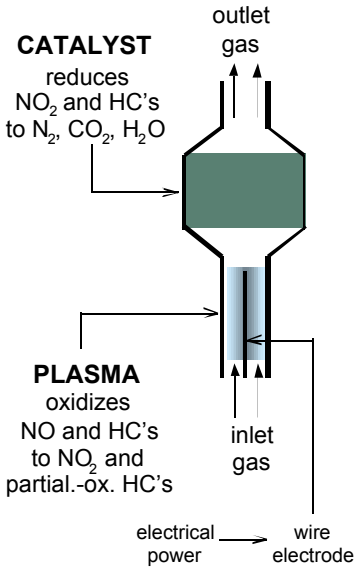

Figure 1. An embodiment of the Plasma-Assisted Catalytic Reduction (PACR) system developed at Lawrence Livermore National Laboratory. U.S. Patent No. 5,711,147. Issued January 27, 1998.

The PACR process makes it possible to improve the activity and durability of catalysts for NOx reduction in diesel engine exhaust. Furthermore, the PACR process enables the use of catalysts that require little or no precious metals, thus providing a potentially cheaper technology for achieving compliance to NOx emission reduction.

Accomplishments

Lead-in work at LLNL supported by DOE-ER and Cummins Engine Company demonstrated fairly efficient reduction of NOx by the PACR process using propene as the reductant. Notwithstanding reasonably favorable economic projections for such a treatment process, the use of propene would require an extra logistical trail. The SERDP project in FY98 was proposed with the intent of determining the feasibility of replacing propene with JP-8 or diesel fuel, which would eliminate the extra logistical requirement. A diesel generator typical of aircraft ground support equipment was selected as a source of NOx. FY98's target—to demonstrate feasibility of the PACR process with a lab prototype system treating real diesel exhaust with diesel fuel as the reductant—was accomplished in three steps: Upgrading the test stand to accommodate a 200-slpm slipstream of exhaust, demonstrating efficient NOx reduction by propene, and further upgrading of the test stand and diagnostic instruments to accommodate delivery of liquid fuels. Diesel fuel proved a less-reactive reductant than propene; nevertheless, the project demonstrated attainment of the regulatory requirement of $\geq$50% NOx removal at an operating criterion of $\leq$5% net fuel penalty at both bench and pilot scale.

FY99's targets were to design and construct a full-scale [9000 slpm] prototype PACR control device, and to integrate HC and soot catalysts into the control system. This major milestone was also achieved. A full-scale NO_x control system was completed and successfully operated to treat the full exhaust flow from a Cummins 100-kW diesel engine generator set. The entire full-scale NO_x control system, including diagnostics, was successfully operated on the engine test stand. All of the elements needed to do quantitative lifetime testing were incorporated into this full-scale feasibility demonstration, including chemical analysis of effluents. The results from the full-scale tests were consistent with scaling predictions based on previous bench scale and pilot scale tests. Figure 2 shows photographs for the full-scale PACR device connected to a Cummins B-series diesel engine.

The first full-scale unit was designed to facilitate disassembly and reassembly during the durability and optimization phase in FY00. We have conceptualized what a smaller, more compact PACR unit might look like for mobile applications. One concept that is very promising is shown in Figure 3.

Benefit to DoD

The use of plasma-assisted catalytic reduction for NOx emission control would enable DoD to operate its diesel engines in a cleaner manner. The technology will improve defense readiness by reducing DoD operational impediments caused by commitments to

(a) (b)

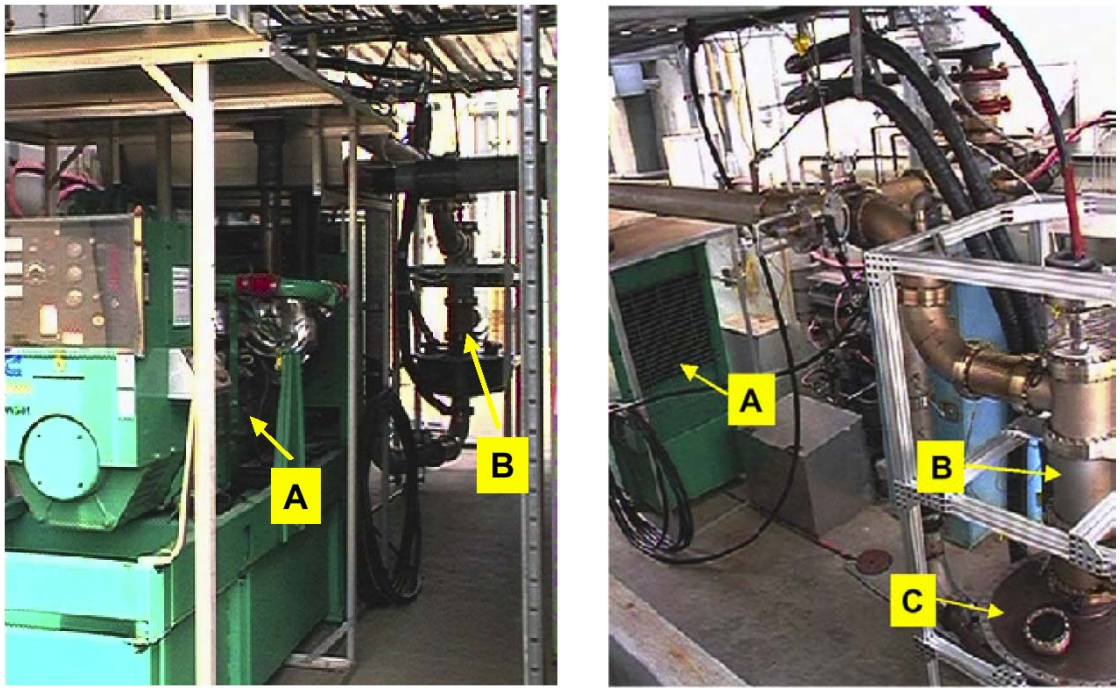

Figure 2. (a) Photograph of the Cummins B-series diesel engine generator set used for testing the PACR device. A: diesel engine; B: PACR device. **(b)** Photograph of the piping between the diesel generator and the PACR device. A: Back of the diesel generator; B: housing for plasma processor; C: housing for NO_x reduction catalyst.

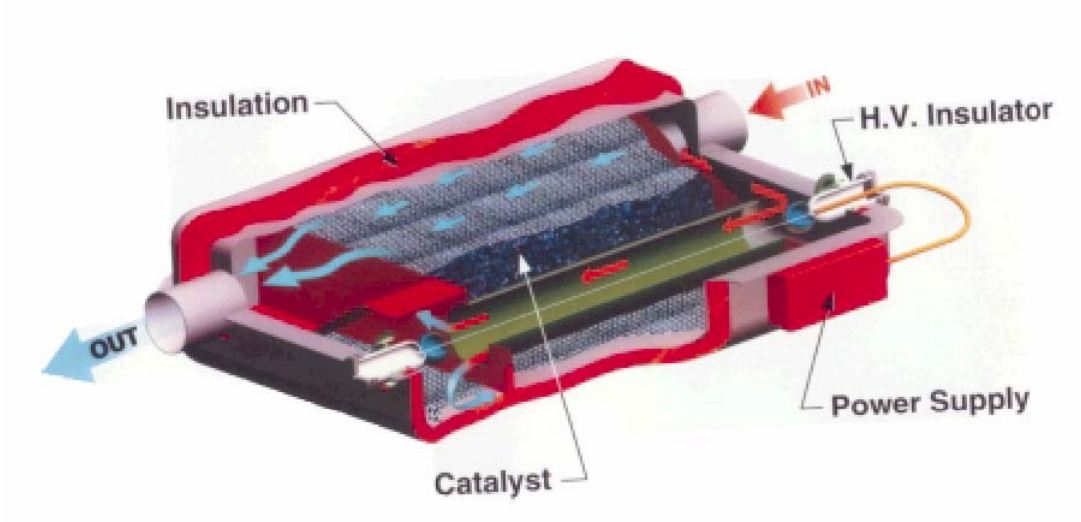

Figure 3. Conceptual design for a compact PACR unit integrating both the plasma processor and the catalyst bed in a single housing.

environmental regulations. For example, drastic decreases in NOx emissions from diesel-powered aircraft ground support equipment (AGE) are being required at U.S. Air Force bases. Data on diesel AGE emissions testing show that the NOx emissions from these generators are around 5 g/bhp-hr, depending on the load. The environmental regulations require these emissions to be reduced to less than 2.5 g/bhp-hr. Noncompliance has led to the specification of a logistically disastrous all-electric system that would preclude mobility exercises involving bases and personnel trained in the use of existing AGE components. The mission readiness of important AGE components will depend on the successful development and implementation of advanced NOx aftertreatment technologies. The PACR process proposed here is an innovative technology that shows great potential for meeting this need. The expected benefits throughout DoD will be considerable since DoD makes extensive use of diesel engines for applications including propulsion, heavy duty transport, service electrical power, emergency power, and damage control in the Air Force, Army and Navy.

The technology is predicated on a fail-safe concept, that even catastrophic failure of the control does not impair the function of the operational device. The unit cost and the minimum power consumption are large enough that application to such small devices as leaf blowers, trimmers, lawn mowers, and hand tools seems unlikely to be practical, despite the large relative emission rate from these common sources. The applications immediately available are to stationary and mobile diesel-powered equipment, including aerospace ground equipment, construction equipment, and fork lifts. With minor engineering adaptations, the same technology will be applicable to stationary power turbines, incinerators and boilers. Application to motor vehicles and other nonsteady-state devices is projected, but expected to require additional development to accommodate the frequent variations in engine conditions. Economic evaluations of each of the applications above will determine the practicality of each.

Details of Accomplishments

FY98 Accomplishments

Milestone 1: Install and test liquid hydrocarbon injector in exhaust pipe of Cummins diesel engine generator. Status: Accomplished

The plasma-assisted catalytic NOx control technology is based on the selective partial oxidation of NO (to NO_2) in a plasma, followed by the selective reduction of NO_2 (to N_2) by HCs on a catalyst. The technology has shown very high efficiency for NOx reduction at bench-scale flow rates using real diesel exhaust and using propene as the HC reductant. The HC content of a diesel exhaust is too low for selective catalytic reduction (SCR), and so it is necessary to have a HC additive for post-combustion NOx control. The main objective of Milestone 1 was to characterize the efficiencies for (a) plasma oxidation of NO to NO_2, and (b) catalytic reduction of NO_2 to N_2, when the HC additive used is diesel fuel instead of propene. This is important because it is desirable to be able to use the same fuel for the engine and the NOx aftertreatment.

A liquid HC injector was installed in the exhaust pipe of the Cummins engine. The liquid HC was injected into the full exhaust stream, which had a flow rate of 7600 standard liters per minute (SLPM) and temperature of 350–400 C at an engine load of about 100 kilowatts. A slipstream, typically up to 200 SLPM, of the HC-containing gas stream was directed to the plasma/catalyst deNO_x reactor. A flame ionization detector (FID) was also installed to quantify the C1 concentration of the HC in the gas stream before and after the deNO_x reactor. Two types of liquid HCs have been tested: kerosene and diesel. The efficiencies of these HCs in the plasma-assisted catalysis process have been compared to that of propene. This work is the first test of plasma-assisted catalysis using the same diesel fuel for both the engine and the NO_x control device.

Milestone 2: Characterize power and fuel consumption, and operating temperature window of the PACR process using diesel fuel as the reductant. Status: Accomplished.

A Cummins B5.9 diesel engine running with a 100-kW load was used as the source of NO_x. The engine-out NO_x was 600 ppm. The exhaust temperature was typically between 350–400 C an engine load of 100 kW. A slipstream of the exhaust was fed to the plasma/catalyst processor. The temperature of the plasma/catalyst reactor was independently set at various temperatures to investigate the operating temperature window of the NO_x reduction activity.

Figure 4 shows the NO_x reduction efficiency of the lean-NO_x catalyst at various temperatures as a function of the C1 concentration of the diesel reductant. The plasma was off in this case. One of the major challenges in lean-NO_x catalysis is maintaining high NO_x reduction efficiency at low temperatures with a relatively small amount of HC reductant. A large amount of HC reductant translates into a large fuel economy penalty for the aftertreatment system.

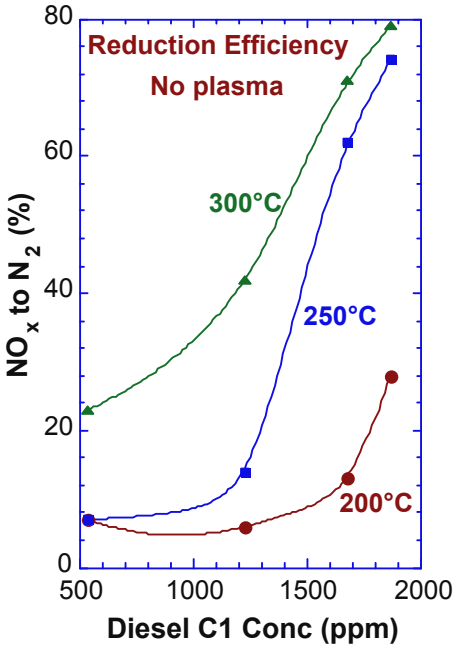

Figure 4. SCR of NOx using real diesel exhaust and diesel reductant. Plasma off. The diesel C1 concentration of 1860 ppm correspond to about 2.5% fuel penalty; *i.e.*, the

amount of diesel fuel needed to accomplish reduction of NOx is 2.5% of the amount of diesel fuel needed to power the diesel engine.
To estimate the fuel economy penalty we rely on the performance report for the Cummins B5.9 diesel engine. For the engine running 1800 rpm at 100 kW, the air flow is 567 kg/hr, and the fuel flow input to the engine is 21 kg/hr. Assuming a fuel molecule composition of $C_{13.3}H_{26.6}$, the fuel flow to the engine corresponds to 42 standard liters per minute (SLPM). The engine exhaust flow is 7600 SLPM. Thus, the number of fuel molecules consumed in running the engine is (42 / 7600) x 10^6 = 5526 ppm. Suppose the lean-NO_x catalyst requires 2000 ppm of diesel based on the C1 concentration. Again assume 13.3 C1 for each diesel molecule. The number of diesel molecules required by the catalyst is (2000 / 13.3) = 150 ppm. The fuel economy penalty is thus 100 x (150 / 5526) = 2.7 %.

The effect of the plasma on NO_x reduction efficiency is shown in Figure 5 for a plasma/catalyst system at a temperature of 250 C and using a diesel reductant C1 concentration of 1250 ppm. The NO_x reduction efficiency is presented as a function of the electrical energy density input to the plasma. The electrical energy density is given in units of Joules of electrical energy per standard liter of gas in the plasma reactor. As a rule of thumb, each 10 J/L of energy density input to the plasma corresponds to a fuel economy penalty of 1 %.

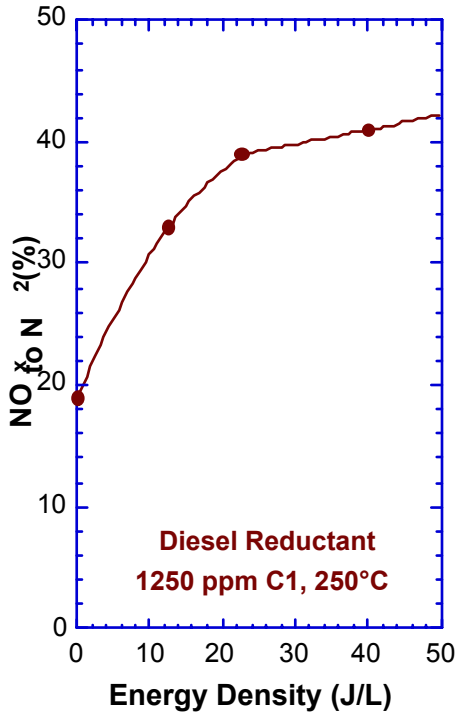

Figure 5. NO_x reduction efficiency of the plasma-assisted lean-NO_x catalyst at 250 C using a diesel reductant C1 concentration of 1250 ppm. The NO_x reduction efficiency is presented as a function of the electrical energy density input to the plasma.

The amount of HC reductant in Figure 5 is relatively low, corresponding to a C1/ NO_x ratio of 2. The data in Figure 5 shows that the NO_x reduction efficiency at 250 C increases by a factor of two when the plasma is given 2% of the engine output power. The effect of the plasma and the diesel C1 concentration on the NO_x reduction efficiency is shown in Figure 6 for a plasma/catalyst system at a temperature of 200 C. At low levels of diesel reductant input, the plasma can significantly enhance the NO_x reduction efficiency. The level of enhancement is proportional to the energy density input to the plasma. The combination of the plasma with a high level of diesel reductant provides very high NO_x reduction efficiency even at the low temperature of 200 C.

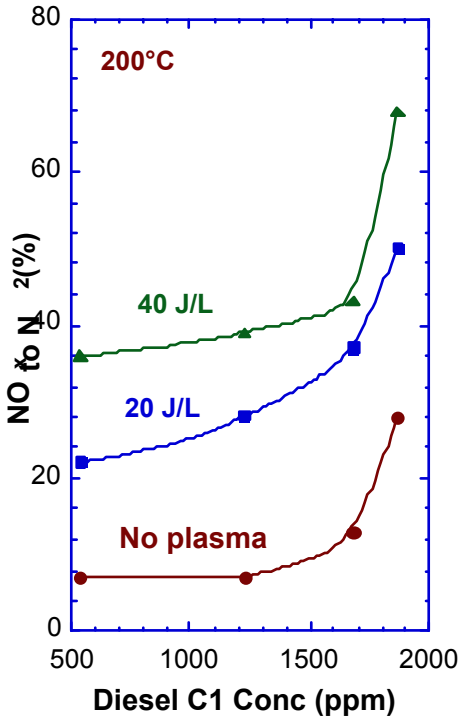

Figure 6. NO_x reduction efficiency of the plasma-assisted lean-NO_x catalyst at 200 C as a function of the diesel reductant C1 concentration. Data taken using a slipstream of the exhaust from a Cummins diesel engine. The NO_x reduction efficiency is presented for three levels of electrical energy density input to the plasma.

The preliminary data using diesel, although very encouraging, indicate that it is not as good as propene. The plasma oxidation efficiency using diesel is comparable to that using propene; however, the SCR efficiency is up to a factor of two lower using an equivalent hydrocarbon C1 concentration. Nevertheless, high efficiencies for NOx reduction have been observed even with diesel when the concentration was sufficiently high. Up to 80% NOx reduction has been observed when the diesel reductant injected into the deNOx reactor is only 2.5 percent of the diesel fuel used by the engine.

The catalytic chemistry of NOx reduction using diesel is apparently different compared to propene. However, there is the possibility that part of the decreased activity using diesel

as the HC reductant can be attributed to our inexperience with the hardware used for liquid HC injection. There is some experience by Cummins that if diesel fuel is correctly mixed into the exhaust gas, the effectiveness of diesel fuel can be almost as good as propene. These results were achieved only after carefully reworking the liquid injection hardware. Other options for optimizing the injection of diesel into the deNOx reactor were subsequently investigated.

Milestone 3: Characterize the effect of SO_2 in the diesel fuel on the NO_x reduction activity. Status: Accomplished.

State-of-the-art lean-NO_x catalysts degrade quickly in the presence of SO_2 in the exhaust. There is a heated debate between engine and oil companies over the need to reduce sulfur (down to 5 ppm or less) in the fuel so that catalyst technologies can efficiently reduce tailpipe emissions of NO_x. The SO_2 in the engine exhaust can poison catalyst activity and also lead to the production of unwanted sulfate particulates. Catalysts that are active in converting NO into NO_2 are also active in converting SO_2 into SO_3. SO_3 adsorbs more strongly on NO_2 adsorption sites and more stably than NO_2, thus degrading the overall NO_x conversion efficiency. By using a plasma to oxidize NO to NO_2 (instead of using an oxidation metal in the catalyst) it may be possible to make the catalyst tolerant to the sulfur in the fuel.

The purpose of these tests is to determine whether or not SO_2 is oxidized during the Plasma-Assisted Catalytic Reduction (PACR) process. Experiments were done using mixtures of synthetic air in various combinations.

1	10% O_2, 500 ppm SO_2, balance N_2
2	10% O_2, 500 ppm SO_2, 500 ppm NO, balance N_2
3	10% O_2, 500 ppm SO_2, 1000 ppm C_3H_6, balance N_2
4	10% O_2, 500 ppm SO_2, 500 ppm NO, 1000 ppm C_3H_6, balance N_2
5	10% O_2, 5% H_2O, 500 ppm SO_2, balance N_2
6	10% O_2, 5% H_2O, 500 ppm SO_2, 1000 ppm C_3H_6, balance N_2

The tests were conducted using SO_2 levels larger than what is normally expected from typical diesel fuel. The plasma energy density was set to around 40 J/L. If no oxidation effect is discovered using these reaction conditions, then it is not likely that milder conditions will present a different outcome, so this can be considered a worst case scenario. The tests were repeated multiple times to gain statistical significance. SO_3 was never directly detected in any of the experiments, so the production of SO_3 can be inferred only indirectly from the disappearance of SO_2.

The characterization method employed in this study is FTIR. There are two possible ways to determine whether the plasma is affecting the SO_2 content. One is to examine the effluent from the processor and see if any SO_3 is formed. If it is assumed that the level of SO_3 formation is at or near zero, then the spectrometer may not be able to detect small amounts of SO_3. The other method is to see if the SO_2 level is reduced beyond a point that could be attributed to statistical measurement error. If the repeatability of SO_2

detection is good enough, it may be possible to infer a very low concentration of SO_3 formation indirectly. This indirect SO_2 characterization method was employed in our analysis.

Figure 7 shows the IR spectrum for SO_2. There are two peak envelopes available for characterizing SO_2. One is located at approximately 1361 cm^{-1} (*Q* branch) and the other is located at approximately 1136 cm^{-1}. The 1361 cm^{-1} envelope is a fairly well developed band with *PQR* rotational fine structure. The *Q* branch occurs at approximately 1361 cm^{-1} and is used to label the location of this peak envelope. The chief drawback in using the 1361 cm^{-1} band is its proximity to the water bands. The 1136 cm^{-1} band is about one order of magnitude lower in absorbance compared with the 1361 cm^{-1} band, but does not suffer from the water interference. In this study, only the 1361 cm^{-1} peak is characterized as it affords the best chance for repeatability due to signal strength. The 1136 cm^{-1} band is available for study if needed.

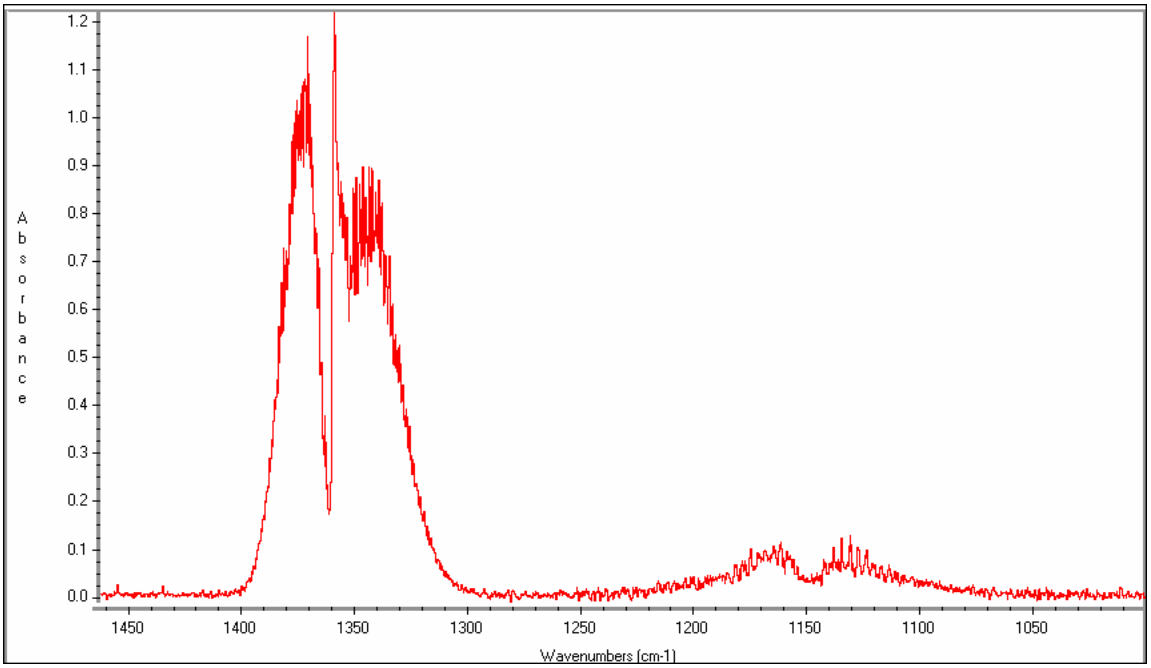

Figure 7. IR spectrum of SO_2 in the gas phase, taken in the processor midport between the plasma and the catalyst.

There are two possible methods to treat the FTIR data in establishing changes in the SO_2 level. One is to use the *Q*-branch peak absorbance as the measure of the concentration of SO_2 in the gas mixture. The other is to integrate the *PQR* band and use the integrated peak intensity. The *Q*-branch method is simple to implement but suffers from more variability because of the varying population of the rotational states giving rise to the fine structure. The integrated band approach should be more repeatable since it averages out the rotational state populations. However, since this band can overlap with water peaks, it is subject to error when water levels are changing.

Real engine exhaust will contain significant amounts of water vapor in the gas stream. The effect of water vapor on the mix of species after plasma treatment can be profound, because water provides the aggressive OH radical in the plasma. Consequently, it was important to understand the effect of water on the oxidation of SO_2. For these tests, a gas mixture of 500 ppm SO_2, 10% O_2, 5% H_2O and balance N_2, in the presence and absence of 1000 ppm C_3H_6 was used with and without plasma.

First, inspection of the IR spectra indicates that it will be impossible to use the 1361 cm^{-1} peak envelope due to interference from the water bands. However, because the SO_2 content is so high, the 1136 cm^{-1} envelope is available to characterize the system. There is slight water interference in this region, but it can be shown that one can subtract out the water bands and obtain reasonable information. Therefore, the data were analyzed using the integrated intensity of the 1136 cm^{-1} band with the integration window defined as being between 1050 and 1250 cm^{-1}. The water bands were subtracted from the sample spectra using a wet syn-air blank that does not have any SO_2 present.

Our conclusions regarding the effect of SO_2 are as follow:

- There is no significant conversion of SO_2 into SO_3 during the PACR process. Under a worst-case scenario of 500 ppm SO_2 and large plasma power, the level of SO_2 disappearance is only around 5%, which is very close to the statistical noise in the measurements.

- Without the HC, there appears to be some oxidation of SO_2 due to OH radicals. These OH radicals are scavenged by the HC required for the PACR process.

- The amount of HC needed for PACR is driven by the NO-to-NO_2 conversion, not by the scavenging process that prevents the SO_2 to SO_3 conversion.

The plasma/catalyst combination is highly effective in controlling NO_x emissions even in the presence of large amounts of SO_2 in the exhaust. Plasma-assisted catalysis is more sulfur-tolerant than catalysis alone. This discovery is especially significant given the heated debate between engine and oil companies over the need to reduce sulfur in fuels in order to reduce tailpipe emissions of NO_x.

Milestone 4. Optimize and characterize liquid HC reductant atomization and mixing. Status: Accomplished.

The original method of introduction of liquid reductant into the diesel exhaust stream, installed in Milestone 1, was through an injection system positioned within the engine exhaust line. The diesel reductant was injected into the full exhaust flow.

There were two problems encountered in the use of a diesel reductant.

First, the data using diesel fuel indicate that it is not as good a reductant for NO_2 as propene is. The plasma oxidation efficiency using diesel fuel was comparable to that

using propene; however, the SCR efficiency is up to a factor of two lower using an equivalent hydrocarbon C1 concentration.

Second, we observed a disparity between the diagnostic reading from the flame ionization detector (FID) and the calculated concentration of HC based on the injected amount. For some reason, the FID reading always indicated a HC content in the gas stream lower than the amount calculated from the setting of the high-pressure fuel injector. Various reasons for this disparity were investigated, but none of them have been conclusively identified as being the culprit.

A new liquid HC injection system was put into place to address both of the above problems. The new injection system used a liquid HC evaporator, and the HC vapor was introduced into the slipstream flow immediately before the plasma/catalyst reactor. This design provided closer control of delivery rates and better management of loss mechanisms.

Because of the high flow rates of HC expected, the FID ran in a non-linear regime. The roll-off response of the FID at high HC concentrations was likely a symptom of a saturated electrometer detector. As we wanted to know something about the absolute amounts of HC as well as to compare the two injection schemes, a calibration of the non-linearity was done. A single-point calibration using 1000 ppm CH_4 in N_2 was performed. A multi-point calibration using mixtures of C_3H_6 in N_2 was also performed.

Figure 8 shows the non-linear nature of the FID response, using mixtures of C_3H_6 in N_2. The FID response tends to roll off as the input HC concentration increases. To correct for the non-linearity, the data were plotted with the input concentration of the HC as the dependent variable. A non-linear regression analysis was then performed to provide coefficients such that the FID reading could be corrected and the true HC content determined. A third-order polynomial fit was applied to the data shown in Figure 8, and the resultant coefficients are shown on the plot.

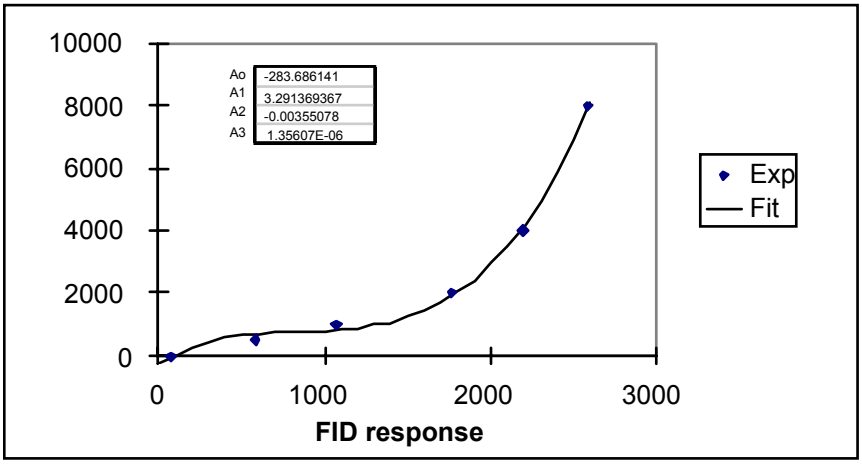

Figure 8. Non-linear FID response to mixtures of C_3H_6 in N_2.

A comparison between the original injection scheme and the new injection scheme is shown in Figure 9. The two injection schemes showed surprisingly consistent behavior. The FID response shown in Figure 9 is simply the FID reading without taking into account the non-linearity of the FID in coming up with the true HC content. However, an examination of the calibration curve and the non-linear fitting shown in Figure 9 indicates that the adjustment to the FID reading to render a true HC content was very small and could be neglected.

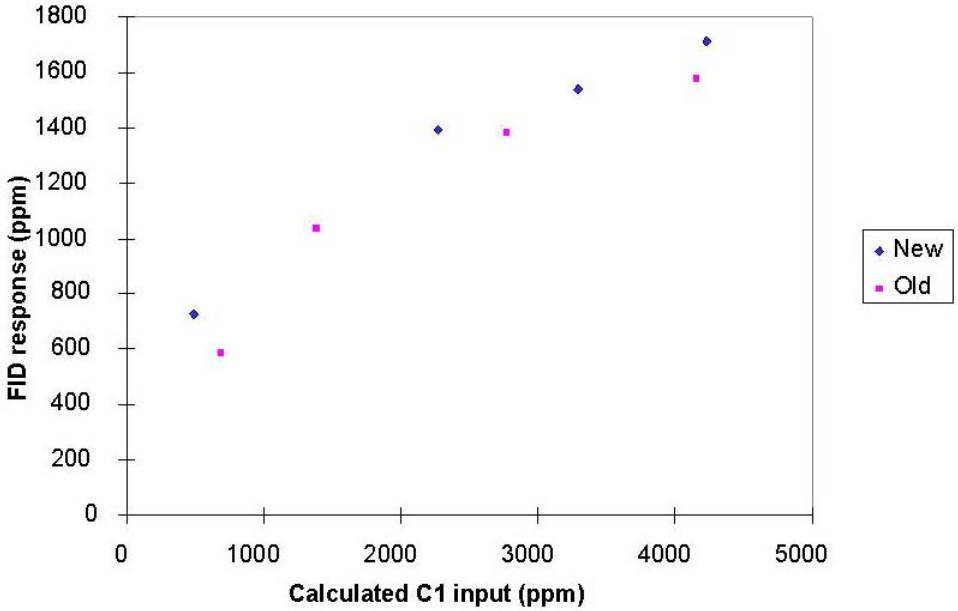

Figure 9. Comparison between the original and new injection schemes.

The two HC injection methods gave very similar results across the wide range of HC input concentration. This suggested that there is something inherent in the injection of diesel, regardless of method, that leads to significant disparities between the calculated injected amount and the amount as detected by the FID.

With the new injection method, the efficiency of oxidation of NO was still as good as for propene, and the efficiency of reduction of NO_2 was still about half that of propene. This confirmed that the chemistry of the larger HCs on this SCR catalyst is less favorable than that of propene under our test conditions, and that the point of delivery is not a prominent factor in determining the course of the system chemistry. Additional experiments are planned to examine the effect of changing exhaust flow rate, and the effectiveness of individual, pure fuel constituents, *e.g.*, pentadecane, as a reductant.

Summary Regarding Milestones 1–4

The work described Milestones 1–4 revealed that the HC reductant type has a large effect on the NO_x reduction efficiency. The reduction efficiency depends not only on the pre-catalyst HC level, but also on the pre-catalyst HC composition. The chemistry of the heavier HCs on the SCR catalyst is inherently different and less efficient than that of propene. To preserve the option to use the engine fuel as the reductant, we planned to

explore the effect of varying conditions in an attempt to optimize the speciation of diesel in the plasma reactor. Pre-catalyst cracking of the diesel fuel to smaller alkenes and other partially oxygenated HCs could potentially be important.

Next we designed and built a pilot-scale NO_x treatment system to accommodate 1500 SLPM of exhaust gas flow from the Cummins B5.9 diesel engine, an order-of-magnitude scale-up from the bench-scale prototype used in the previous studies. NO_x reduction efficiency was characterized as a function of engine power consumption, fuel usage, and exhaust flow rate through the deNO_x reactor. These data were used in an engineering cost estimate for a full-scale system and to determine the extent of control possible.

FY99 Accomplishments

Milestone 5: Develop a plasma processor capable of 9000 SLPM flow and 5 kW power. Status: Assembly of the full-scale plasma processor unit completed.

Our baseline for full-flow testing of the Cummins B5.9 diesel engine generator set was based on a maximum flow of 8760 SLPM at 100% load on the engine. We had established that an energy density of about 20 J/L is required for the plasma processor. This required a plasma processor capable of exciting the plasma with at least 3000 watts.

A sketch of the processor is shown in Figure 10. The electrical connections were made at the screened end. The screen created a Faraday cage so that electromagnetic radiation is minimized. The alumina tube that forms the dielectric barrier wss supported on the two flanges of the center spool piece. A screen to prevent electromagnetic interference also covered the gas ports.

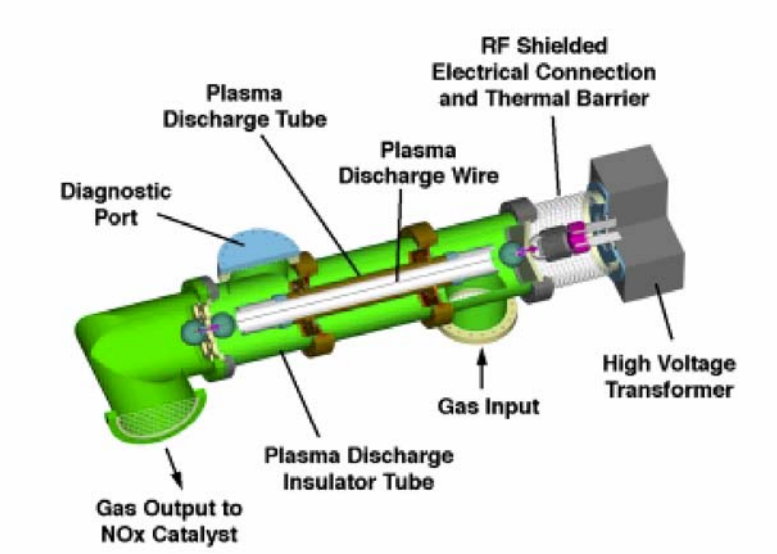

Figure 10. Sketch of the plasma processor. Electrical connections are made at the right end, inside a screen that creates a Faraday cage to minimize electromagnetic radiation. Flanges on the center spool piece support the alumina tube forming the dielectric barrier. A screen to prevent electromagnetic interference also covers the gas ports.

Milestone 6: Develop catalyst system to treat 9000 SLPM flow. Status: Design and assembly of the full-scale catalyst bed unit was completed.

A critical issue in the design of the catalysts system was the effect that back pressure caused by the catalyst bed would exert on engine performance. The means for holding the catalyst was required to minimize back pressure on the engine. A series of measurements were taken to quantify the amount of back pressure that could be allowed. From these data, the depth and aspect ratio of the catalyst were then determined.

We deployed about a 10-inch-deep catalyst bed in our test stand and measured the pressure drop, which was relatively small. Accordingly, we felt comfortable designing the catalyst bed at least 10 inches thick. More work remains to characterize the HC utilization over this thickness. Ideally, we wanted to have a catalyst bed deep enough to use up the HCs to minimize slip but not so deep that not enough HCs survive to promote the reduction chemistry.

After the catalyst holder was completed and parts were fabricated, we decided to use a support frame/monorail as a means of lifting the catalyst holder or plasma processor in and out of the system.

We also continued to test alternate catalyst structures. We tested a structure involving a catalyst washcoated on a filter-type monolithic platform. The filter platform had a unique advantage in that every adjacent pair of channels of the monolith is plugged at opposite ends, thus forcing gas to flow across channels, through the porous structure of the monolith. It was expected that forcing the gas to flow through porous structure bearing a thin washcoat of the catalyst, would enhance contact of the gas with the catalytic material, thereby effectively decreasing the volume requirement for the catalyst system. The result with the filter-type monolith did not show a significant enhancement in NO_x reduction efficiency compared to a catalyst pellet bed operating at the same gas flow rate and catalyst volume. This indicates that, under our operating conditions, the NO_x reduction efficiency is kinetically limited and not mass-transfer limited. The flow-rate-to-catalyst-volume ratio at which we were operating afforded sufficient contact between the gas and the catalyst surface. The important quantity was the residence time of the gas molecules on the catalyst surface. Increasing the residence time required either decreasing the gas flow rate or increasing the catalyst volume.

The second means of increasing the effectiveness of the catalytic material was to enhance its fundamental properties. We tested a new zeolite catalyst provided to us by Engelhard. At the relatively low temperature of 200 C and using kerosene as the reductant, the new catalyst showed NO_x reduction efficiency a factor of two better than our present metal-oxide catalyst. The activity persisted up to 5% water vapor level in the exhaust, and then degraded rapidly as the concentration of water vapor continued to rise. The water vapor content of the exhaust from our Cummins B5.9 diesel engine is shown in Figure 11 as a function of the engine load. We worked with Engelhard to understand the water threshold effect of the zeolite catalyst. We planned to do some characterization to establish any possible hydrothermal stability or transient adsorption problems with this zeolite.

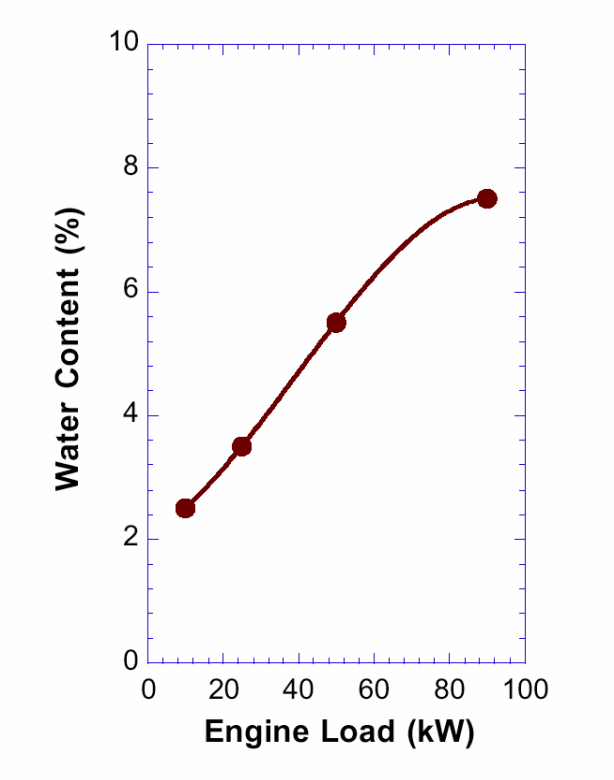

Figure 11. Water vapor content of the exhaust from the Cummins B5.9 diesel engine. Higher engine load leads to higher water content in the exhaust. The NO_x reduction efficiency of all catalysts we tested showed high sensitivity to the water content of the exhaust. This was true for both conventional SCR and our PACR process.

We also performed additional characterization experiments on our present metal-oxide catalyst as a function of engine load, using kerosene as the reductant. These pilot-scale experiments were done to closely simulate the conditions we expected from our full-scale prototype. Figure 12(a) shows the data taken using the exhaust from the Cummins B5.9 diesel engine at 50 kW load. Engine-out NO_x was around 500 ppm at the 50-kW load. Kerosene was used as the HC for NO_x reduction. The catalyst temperature was 300°C. For the same amount of kerosene reductant flowing through the catalyst bed, the plasma dramatically enhanced the NO_x reduction efficiency. Figure 12(b) shows the data taken using the exhaust from the Cummins diesel engine at 90 kW load. Engine-out NO_x was around 670 ppm at the 90-kW load. The maximum NO_x reduction efficiency at higher engine loads was slightly less because of the higher level of water vapor in the exhaust.

If the new zeolite catalyst proved as durable as our metal-oxide catalyst, we had expected to achieve a much higher maximum NO_x reduction efficiency at a lower temperature for the same catalyst volume. In the meantime we designed the full-scale catalyst bed to work with the simple metal-oxide material because (a) we had more data on its durability, (b) it is a much cheaper catalyst, and (c) we had large quantities of it in hand.

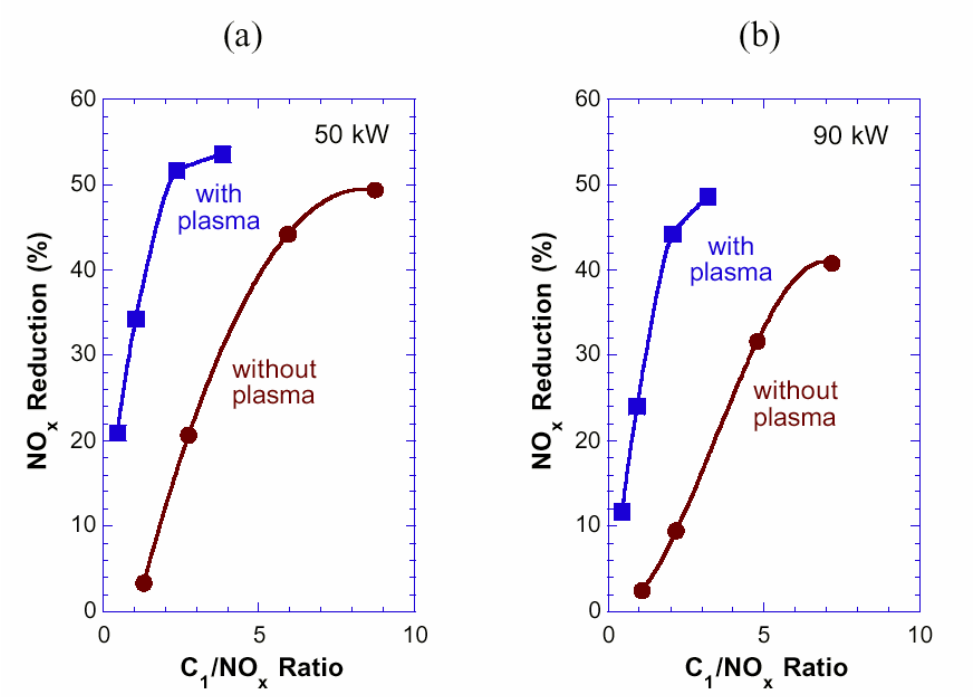

Figure 12. Pilot-scale tests done to closely simulate the conditions we expect from our full-scale prototype. (a) Data taken using exhaust from Cummins diesel engine at 50 kW load. Engine-out NO_x was around 500 ppm. (b) Data taken using exhaust from Cummins diesel engine at 90 kW load. Engine-out NO_x was around 670 ppm. Kerosene was used as the HC for NO_x reduction. Catalyst temperature = 300°C. Metal-oxide catalyst.

Milestone 7: Integration of the catalyst bed with the plasma processor. Status: Integration of the full-scale PACR unit was completed.

A full-scale NO_x control system was completed and successfully operated to treat the full exhaust flow from a Cummins 100-kW diesel engine generator set. The generator used for testing is typical of aircraft ground support equipment, and representative of medium-sized diesel engines used by DoD to power mobile and stationary heavy equipment.

Installation of the piping, plasma processor, and catalyst bed was completed. The engine was operated at up to maximum capacity and the pressure drops across the major components were measured.

Installation of the heated lines for sampling the gas mixtures was completed. Insulation was also installed for the piping from the diesel engine to the plasma processor and catalyst bed. Additional diagnostics, such as orifice flow gauges, were installed in the exhaust line.

The entire full-scale NO_x control system, including diagnostics, was successfully operated on the engine test stand. All elements needed to do quantitative lifetime testing were incorporated into this demonstration, including chemical analysis of effluents.

Exhaust from the diesel engine was pulled into the full-flow processor (FFP) and the NO_x level measured. The exhaust was sampled using the new heated line assembly for the FFP at both "midport" (after the plasma processor) and the "outlet" (after the catalyst bed).

When the initial test run was commenced, the system behaved as expected. A small amount of NO_x removal, around 5 percent, was observed in the absence of kerosene. This may be due to a small amount of absorption or due to the presence of low but detectable amounts of HC in the exhaust stream coming from the engine itself. When kerosene was injected into the exhaust stream, NO_x removal commenced and was improved upon addition of the plasma. An initial removal figure of approximately 55 percent was found for these conditions. This result is consistent with previous bench-scale and slipstream tests that demonstrated attainment of DOE's criterion for heavy-duty diesel engines of achieving at least 50 percent NO_x removal at no more than 5 percent net fuel penalty.

Figure 13 is a diagram of the full-scale PACR device connected to a diesel generator. The diagram shows the relative sizes of the various components in the test stand. Note that the full-scale PACR device is about the same size as the muffler. The PACR device can be designed so that it also serves as a muffler. The location of the PACR device was constrained by the location of the stack pipe in the adjacent building. The piping between the diesel engine and the PACR device was insulated to keep the temperature in the PACR device as close as possible to the exhaust temperature near the engine.

Figure 14(a) shows a diagram of the PACR device, while Figure 14(b) shows a cutaway diagram of the device. Note that the actual size of the plasma processor is much smaller than its housing. The housing was designed to accommodate different sizes and types of plasma reactors. Figure 14(c) shows a photograph of the full-scale PACR device mounted on the support frame.

Figure 2(a) [on page 4] shows a photograph of the Cummins B-series diesel engine used for testing the PACR device. Figure 2(b) shows a photograph of the piping between the diesel engine and the PACR device. The piping of the PACR device, as well as the high-voltage cable, RF shielding and plasma processor housing, are featured in the photograph in Figure 15.

Figure 16 shows the NO_x reduction efficiency in the full-scale PACR device using kerosene as NO_x reductant. The engine load in this test was 50 kW. The catalyst temperature was 250°C. The engine-out NO_x was around 450 ppm. The amounts of kerosene used corresponded to a C_1/ NO_x of 4 and 7. The results of the full-scale test are consistent with the results obtained in the pilot-scale tests. The plasma dramatically increases the NO_x reduction at lower values of C_1/NO_x; *i.e.*, with less HC.

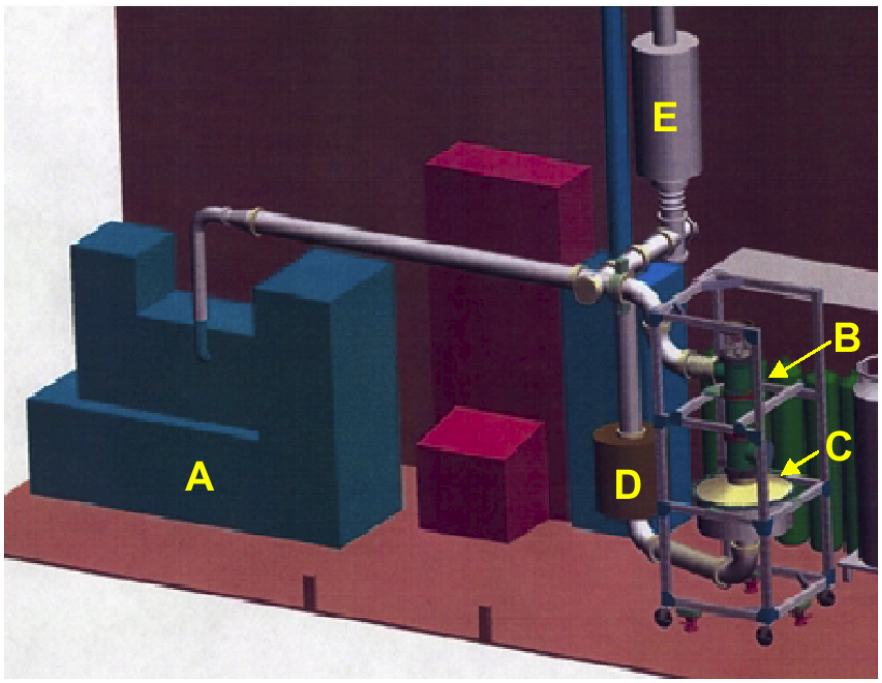

Figure 13. Diagram of the full-scale PACR device connected to a diesel generator. A: 100-kW diesel generator; B: housing for plasma processor; C: housing for NO_x reduction catalyst; D: optional soot/HC oxidation catalyst, E: optional muffler. The location of the PACR device was constrained by the location of the stack pipe in the adjacent building. The piping between the engine and the PACR device was insulated to keep the temperature in the PACR device as close as possible to the engine exhaust temperature.

(a) (b) (c)

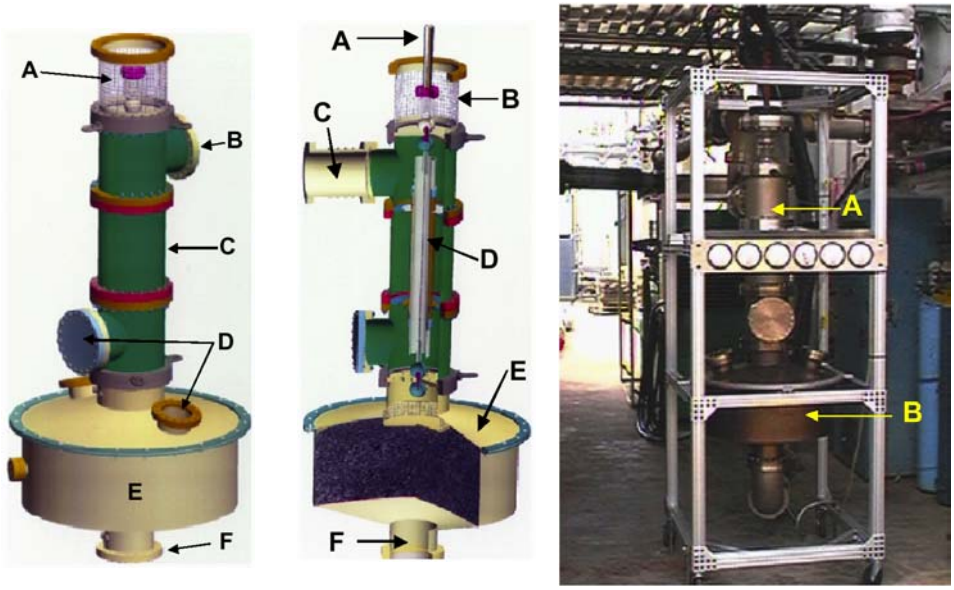

Figure 14. **(a)** Diagram of the PACR device. A: RF shielding; B: gas inlet; C: housing for plasma processor; D: diagnostic and viewing ports; E: housing for NO_x reduction catalyst; F: gas outlet. **(b)** Cutaway diagram of the PACR device. A: high-voltage cable; B: RF shielding; C: gas inlet; D: plasma processor; E: NO_x reduction catalyst; F: gas outlet. Note that the actual size of the plasma processor is much smaller than its housing. The housing was designed to accommodate different sizes and types of plasma reactors. **(c)** Photograph of the full-scale PACR device. A: housing for plasma processor; B: housing for NO_x reduction catalyst.

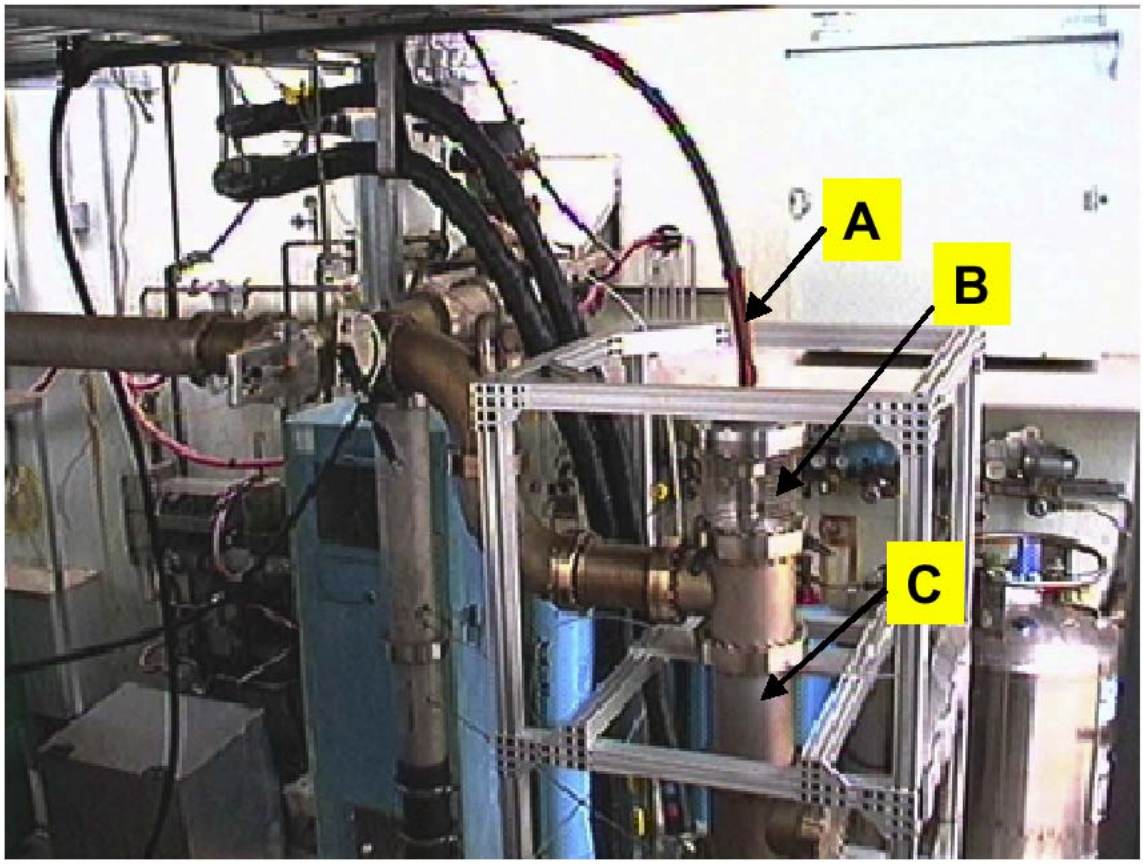

Figure 15. Photograph of the cabling and piping of the PACR device. A: high-voltage cable; B: RF shielding; C: housing for plasma processor.

Milestone 8: Engineering cost estimate for a full-scale system Status: completed.

Table 1 shows the engineering cost estimate for the PACR device, including power supply and soot filter. The total cost depends on the number of units. The estimate is based on actual experience on the full-scale system that we recently built and installed. The flanges in the test system were designed to facilitate disassembly and reassembly during the durability and optimization phase in FY00. The flanges will not be necessary in a commercial system. The ceramic components are used mainly for high-voltage insulation.

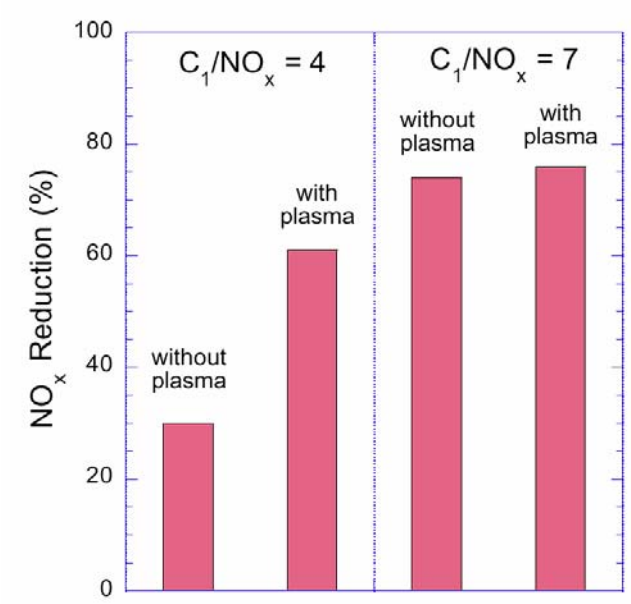

Figure 16. NO_x reduction efficiency in the full-scale PACR device. Engine load = 50 kW. Catalyst temperature = 250°C. Engine-out NO_x was around 450 ppm. The amount of kerosene used as the NOx reductant corresponds to a C_1/NO_x of 4 and 7. The plasma significantly enhanced the NO_x reduction at lower C_1/NO_x.

Table 1

		a	b	c	d	e	f
	Description	**For 1 - 10**	**10-100**	**100-1,000**	**1,000 - 10,000**	**10,000 - 100,000**	**over 100,000**
1	Power Supply	2,500	2,125	1,535	250	181	131
2	Ceramic Components	1,500	1,275	921	175	126	91
3	Catalyst	1,193	1,014	733	175	126	91
4	Plasma Processor*	1,575	1,339	967	125	90	65
5	Soot Filter	736	626	452	150	108	78
6	Assembly & Test	2,750	1,500	1,084	75	54	39
	Total Cost	**10,254**	**7,878**	**5,692**	**950**	**686**	**496**

Notes:
* Welded Structure
a Totally manual operation; same as current design but without the flanges
b Same design; add some fixture set up
c Change design to integrate components;
build molds for ceramic parts, and tooling for metal parts
d Mass produced power supply; purchase catalyst in bulk quantities;
build tools and dies for manufacturing and assembly
e Value engineer components; quantity discount in purchased parts
f Automated production and assembly; quantity discount.

NOx reduction. Because the NOx reduction catalyst we used did not contain any transition metal that would normally efficiently oxidize HCs, a significant fraction of the HC was not reacted. For the 50-kW test, 150 ppm of kerosene was introduced into the PACR device. At the PACR outlet, 69 ppm of kerosene was left unreacted. An HC/soot oxidation catalyst (from Cummins) was therefore used downstream of the PACR device to minimize the HC and soot emissions. The oxidation catalyst removed 75%–80% of the HC slip; thus, around 17 ppm of kerosene went to the stack. We did not have equipment to provide a quantitative measure of the soot emission. The soot particles comprised (roughly equally) a dry carbonaceous fraction and an HC liquid known as the volatile organic fraction. The specification on the HC/soot oxidation catalyst states that it removes 60% of the volatile organic fraction of the soot particles. We had hoped to investigate increasing soot removal by using the plasma to electrostatically trap soot particles and then thermally oxidizing the dry carbonaceous fraction by operating the plasma occasionally in the arcing mode.

FY00 Accomplishments

Power Consumption

Summary: The power consumption in the plasma is actually beneficial for the A/M32A-86 diesel generator!

Emissions control schemes that increase the electrical power consumption of AGE diesel generators are desirable. Plasma-based emissions control schemes will result not only in reduction of emissions but also in fewer engine maintenance problems. Increasing the power consumption will reduce the problem of "wetstacking," which is a major cause of maintenance problems in AGE diesel generators.

Wetstacking is the accumulation of unburned diesel fuel and carbon residues in the engine and exhaust system of diesel engines, including the generator sets used by the military. This leads to cooler-, but rougher-running engines and increased vibration. According to the DoD Project Manager for Mobile Electric Power (PM/MEP), approximately 60-70% of maintenance problems are directly attributable to wetstacking (see http://www.pmmep.org/problem.htm).

The principal cause of "wetstacking" is generator underloading; *i.e.*, running the generator sets at loads 50% below the rated load. According to PM/MEP, the diesel generator sets are frequently operated within 10–20% of the recommended capacity. For example, the A/M32A-86 diesel generator used by the US Air Force can generate up to 200 amps. However, the generator is nominally operated at around 20–30 amps. One of the solutions recommended by PM/MEP to reduce wetstacking is to increase power consumption to above 50%, preferably 70% or higher. This will cause the engines to run hotter, improve combustion and reduce vibration. Doing so will result in fewer engine maintenance problems. While unnecessary in combat situations, using load banks at local maintenance facilities is recommended. The plasma-based emissions control device can

be designed to take the place of a load bank, thus improving engine performance while at the same time reducing emissions of NOx, soot and unburned fuel.

One important result we have derived from our experiments is a predictive model for the power consumption and HC consumption in the plasma. The key to plasma-assisted catalysis is the selective partial oxidation of NO to NO_2. Electrical power is obviously required to produce the plasma. However, the presence of HCs also serves several important functions in the plasma. The HCs minimize the formation of acid products. The HCs also suppress the oxidation of SO_2; oxidation of SO_2 leads to formation of ultrafine particulates and sulfate poisoning of catalyst sites. NO-to-NO_2 oxidation efficiency in the plasma may be expressed as a function of only two variables: (a) the specific energy density (in units of kJ/g(NOx)), and (b) the C1/NOx ratio (*i.e.*, HC-to-NOx ratio). Figure 17 shows a contour plot of the plasma oxidation efficiency as a function of the specific energy density and C1/NOx ratio.

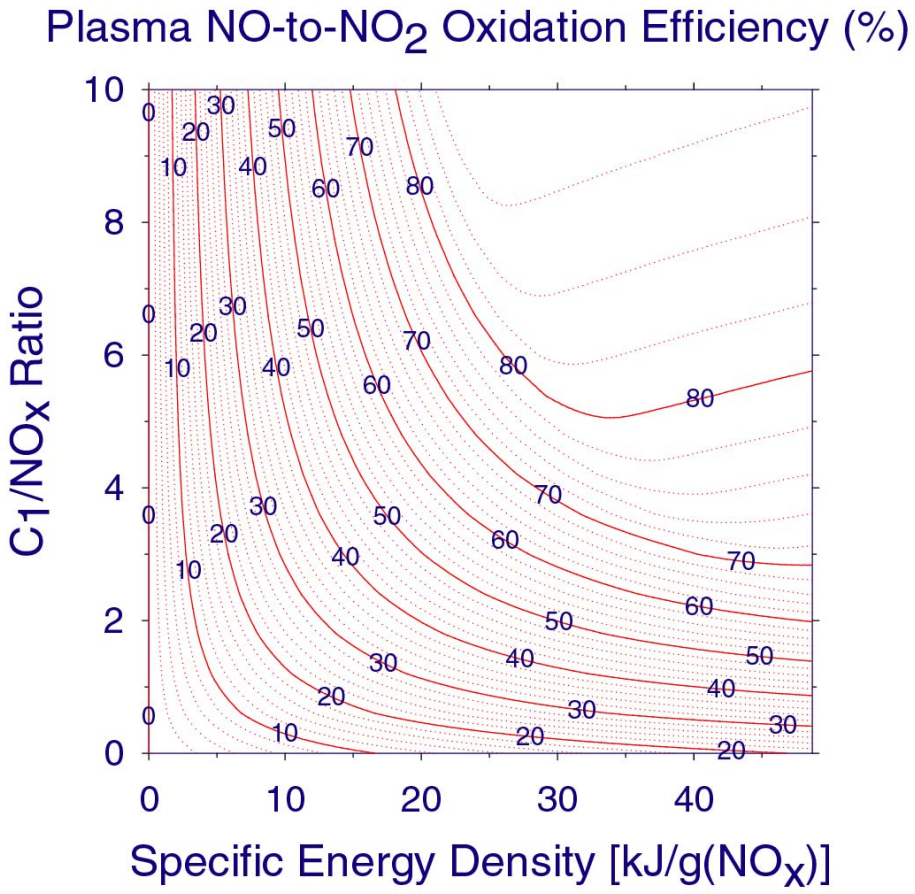

Figure 17. Contour plot of NO-to-NO_2 oxidation efficiency in a plasma as a function of the specific energy density and C1/NOx ratio.

High plasma oxidation efficiency in the plasma can be obtained with either high HC consumption and low power consumption, or low HC consumption and high power consumption. For example, to obtain 70% efficiency, one can use either C1/NOx ratio of 10 and specific energy density of 15 kJ/g(NOx), or C1/NOx ratio of 3 and specific energy

density of 50 kJ/g(NOx). Based on the discussion above, it is now clear that the strategy should be to use low amounts of HC additive with high amounts of power consumption. Given the NOx emission rate, for example in units of g(NOx)/hr, one can use Figure 17 to easily determine the power required by the plasma to achieve a desired level of oxidation efficiency. For example, for a NOx emission rate of 200 g(NOx)/hr, a specific energy density of 50 kJ/g(NOx) would correspond to a power consumption of 2.8 kW to treat the NOx. Additional power from the generator set output can take care of the soot. We have also investigated plasma schemes for oxidizing the soot to CO_2. By combining plasma-assisted catalytic reduction of NOx with plasma oxidation of soot, we will be able to simultaneously remove NOx and soot from the exhaust.

Milestone 9: Catalyst Durability Testing. Status: Completed.

Summary: Exposure to high-temperature water vapor in the exhaust was identified as a major cause of degradation in catalyst activity. Soot trapped by the catalyst is oxidized by the NO_2 from the plasma. Recommendation: To prevent hydrothermal deactivation, the catalyst should be operated at temperatures less than 400 C, and preferably at 300 C or less.

The NOx reduction activity of our catalyst degraded when exposed to high amounts of water vapor. Prolonged exposure to soot also led to blockage of the active sites on the catalyst. During the catalyst durability testing using the full exhaust flow, we noticed that the catalyst activity could be recovered when the catalyst is exposed to a high temperature (400 C) flow. We wondered whether the recovery was due to oxidation of carbonaceous soot, the removal of chemisorbed water, or both. We therefore performed a series of tests, each starting with fresh catalyst samples, to elucidate some of the issues concerning exposure to water.

The first set of data in Figure 18 shows the performance of a fresh sample of the catalyst at 300 C and C1/NOx of 6. The fresh catalyst has SCR (selective catalytic reduction without a plasma) and PACR (plasma-assisted catalytic reduction, with plasma energy density of 25 J/L) performance of 30 and 60%, respectively. This will be referred to as the baseline condition.

In the second set of data, a fresh sample of the catalyst was soaked in water, superficially dried with a towel, and put into the system for testing. This simulates exposure of the cold catalyst to condensate. The performance without and with plasma is degraded. Keeping the gas stream at 300 C and dry for several hours did not change this result.

In the third set of data, the same catalyst sample was treated with house air (dry) at 400 C for a half-day. The NOx reduction activity with and without a plasma was recovered and almost as good as the fresh sample. This result shows that exposure to liquid water is harmful but recoverable and that there is no irreversible change taking place in the catalyst.

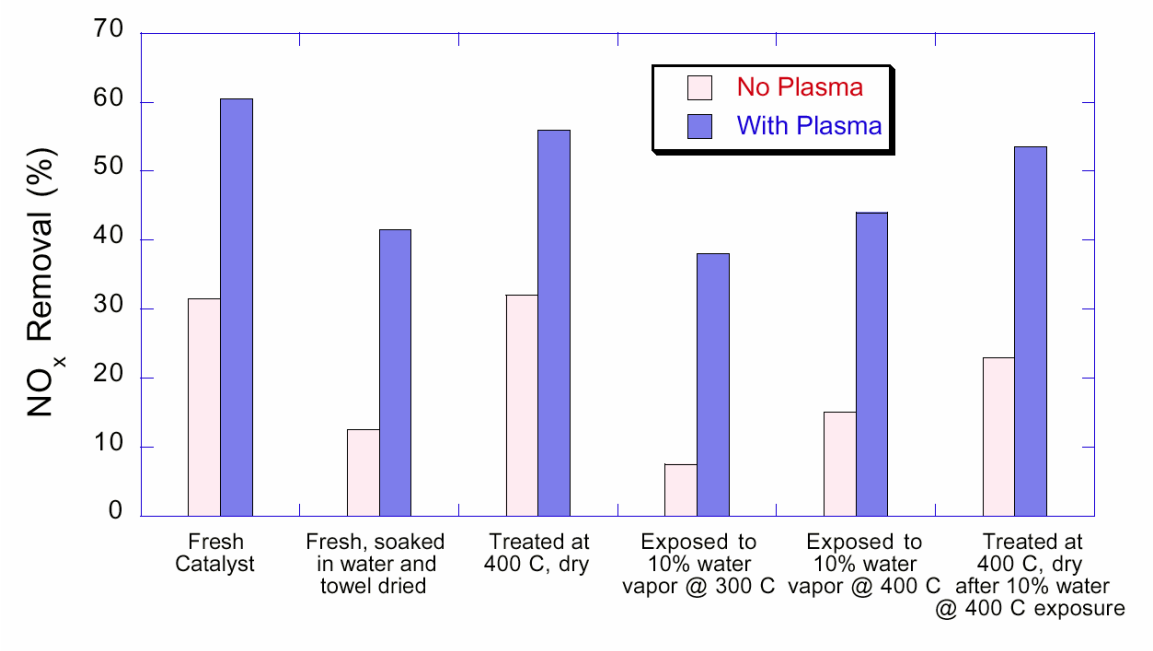

Figure 18. Effect of exposure to water on NOx removal activity.

In the fourth set of data, the catalyst was exposed to 10% water vapor at 300 C and retested. The catalyst performance was reduced to a level very similar to that seen when the catalyst was exposed to liquid water.

Since we know from above that treatment with dry air at 300 C will not change the performance level, one can ask whether treatment with 400 C air laden with water vapor will recover the catalyst. Such a treatment would simulate recovery of the catalyst using engine exhaust at high load levels (with a high water of combustion content). In the fifth set of data, the catalyst was exposed to 400 C air with 10% water vapor for 2 hours, followed by cooling to 300 C in dry air for 1.5 hours. Some partial recovery was observed. In cooling the catalyst for checking under the baseline condition (300 C and C1/NOx of 6), the water vapor was turned off during cooling. This simulates throttling back the engine, where the water level and the exhaust temperature both drop. It is not clear that the recovery in the catalyst is due to that short, dry cooling time. It is also not clear that exposure to 10% water vapor at 400 C has done something irreversible to the catalyst. Both questions were resolved by a dry bakeout at 400 C.

In the sixth set of data, the catalyst sample was treated with dry air at 400 C for several hours in an attempt to complete the recovery of the catalyst and establish whether any irreversible harm was done by exposure to high-temperature water vapor. Although the catalyst performance improved from when a natural cool-down to 300 C occurred, full recovery was not achieved. It suggests that exposure to high water levels at high temperatures causes significant changes to the catalyst function. There are clearly equilibrium and kinetic aspects to this issue. Since SCR is strongly suppressed at 400 C and 10% water, there appears to be a shift towards a hydrated surface that inhibits NOx

removal. If there is indeed a structural rearrangement, then the kinetics of that rearrangement will be important to understanding the lifetime of the catalyst material.

Milestone 10: Plasma Processor Durability Testing. Status: Completed.

Summary: Direct exposure of the soot to the plasma completely oxidized the soot, thus preventing soot accumulation in the plasma region of the processor. However, soot accumulation on the high-voltage insulator plates caused severe localized melting due to arcing. Recommendation: Arcing can be prevented entirely if a pulsed power supply is used. When using a cheaper AC power supply, the electrode in the plasma processor should be designed to minimize high-voltage stress while still providing high average power input. Also consider eliminating the soot upstream of the plasma processor.

Figure 19 shows a diagram of the plasma processor. Note that the actual size of the plasma processor is much smaller than its housing. The housing was designed to accommodate different sizes and types of plasma reactors. The two components of concern with respect to durability are the high-voltage insulators and the dielectric barrier.

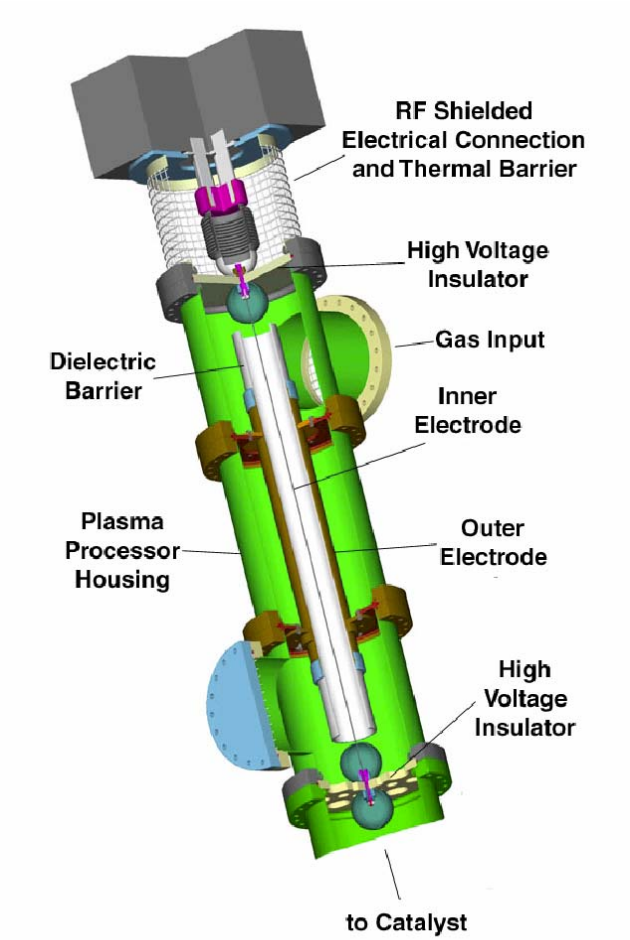

Figure 19. Plasma processor

The plasma processor requires high voltage to operate. High-voltage insulators are needed to provide a means of connecting the center electrode of the processor to the power supply. The soot from the diesel engine can cause the high-voltage insulators to malfunction and arc over much in the same manner that dirt on insulators for ac power lines cause outages.

The need for a dielectric barrier depends on the type of power supply chosen to run the plasma processor. The dielectric barrier is not required if the plasma is driven by very short pulses (nanosecond pulse widths) of high voltage. The use of a pulsed power supply also reduces the risk of failure in the high-voltage insulators. Creation of these very short pulses of high voltage is straightforward but complicated and expensive. The use of a dielectric barrier makes the power supply design much simpler. With the dielectric barrier, the high-voltage pulse width now can be much larger, up to milliseconds or more since the dielectric barrier prevents arcing between the electrodes. Accumulation of soot on the dielectric barrier is a concern because the carbon will act as a conductor and could therefore cause arcing between the electrodes.

Figure 20 shows a picture of the outer electrode and dielectric barrier used in the plasma processor. The dielectric barrier was made of α-alumina. Figure 21 shows a view of the inner surface of the dielectric barrier showing soot in the regions where there was no plasma. Note that the surface is very clean in the region where the plasma was generated. Direct exposure of the soot to the plasma completely oxidized the soot. This result shows that dielectric barrier failure due to accumulation of soot is not a problem. This result also suggests that if we built a trap for the soot, we could regenerate the trap by oxidizing the trapped soot with a plasma.

Figure 20. The outer electrode and dielectric barrier used in the plasma processor.

Figure 21. A view of the inner surface of the dielectric barrier showing soot in the regions where there was no plasma. The surface is very clean in the region where the plasma was generated.

The first set of high-voltage insulators we tried was made of Macor. We chose Macor because it is machinable and can easily withstand very high temperatures (> 1000 C). This material has done a good job in our bench-scale and pilot-scale tests. However, this material is very expensive.

We had a minor setback with the high-voltage insulators during the first operation of the plasma processor with full engine exhaust flow. The insulators that support the center conductor in the plasma reactor cracked, apparently due to mechanical stress from thermal cycling. The insulating plates at the top and bottom of the reactor both cracked after our first day's operation at high temperature. Our analysis of this problem revealed that we mostly overtightened the bolts that "crush" the gasket. This prevented the insulating material from "growing" with temperature resulting in the plate trying to "bubble" outwards, thus cracking the plate. We have since taken steps to minimize the forces on the insulating plates.

We decided to replace the expensive Macor plates with a less-expensive material. We chose a Rescor 914 machinable glass ceramic material made by Cotronics Corp. This new set of high-voltage insulators was installed into the full-flow plasma processor and tested at up to 400 C and up to 22 kV with no breakdown failures. We conducted extensive testing to ensure that the high-voltage insulators can withstand prolonged exposure to engine soot and high-voltage stress. The plasma processor continued to

operate without failure. We then disassembled the plasma processor to examine the components and look at where the soot was accumulating.

Upon disassembly we noticed severe melting on the insulator plate, shown in Figure 22. Soot had accumulated on the plate. The region nearest the inner electrode wire was relatively clean, as we expected because the soot was continually oxidized by the plasma in this region. However, a thick layer soot had built up in the outer regions of the plate. The layer of soot conducted to ground and caused a hot arc to form between the inner electrode and the soot layer on the plate. The arc burned into the insulator plate, melting the plate within, and had started to form a tunnel within the plate. Figure 23 shows a closer view of the melted region in the high voltage insulator. The insulator would have failed if we had continued to operate and the melted tunnel reached the flange.

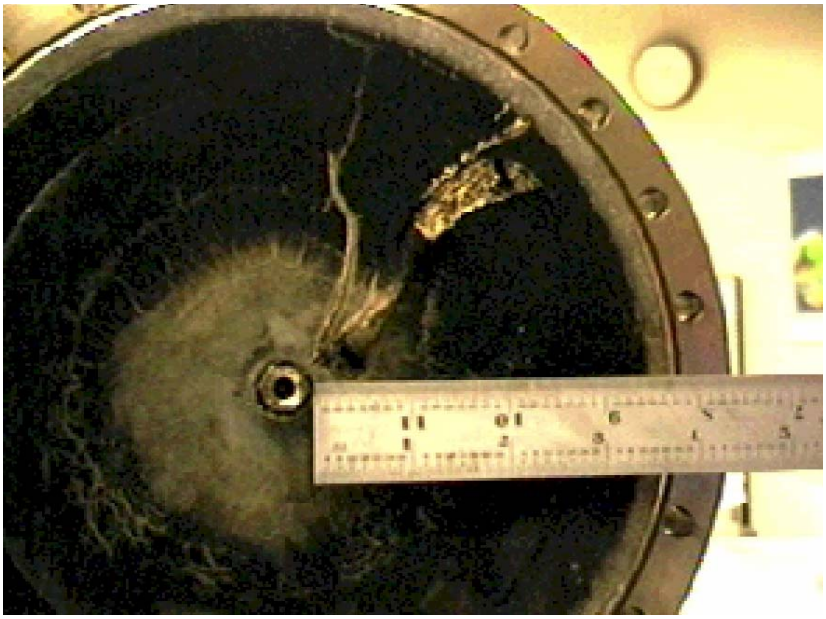

Figure 22. The high-voltage insulator plate of the plasma processor

One way of decreasing the possibility of soot-induced electrical breakdown of the insulator plates is by decreasing the voltage requirement of the plasma processor. This can be accomplished by decreasing the gap spacing between the inner and outer electrodes, and by increasing the field enhancement of the inner electrode. We therefore replaced the wire inner electrode with a finned inner electrode, as shown in Figure 24. The voltage requirement went down as expected and we were able to increase the power density in the plasma using the same power supply. We also tested an inner electrode consisting of a 10-mil wire spirally wrapped around a 1.25-inch-diameter ceramic tube, with a wire spacing of around a cm. This design also decreased the voltage requirement as expected. We are also investigating schemes that would eliminate the soot upstream of the plasma processor.

Figure 23. A closer view of the melted region in the high-voltage insulator

Figure 24. Finned inner electrode used in the plasma processor

Milestone 11: Power Supply Development for Mobile Operation. Status: Completed.

Summary: After extensive power supply development work, a high-frequency AC power supply was successfully used to deliver high power density to the full-flow plasma processor. During the long duration testing of plasma processor, the power supply transformer failed. This led to a rather extensive investigation to understand the failure mode and the requirements for a replacement transformer.

The design of the power supply was linked to the type of plasma processor chosen. The design of the power supply could be significantly simpler than the system tested if we changed our processor type from a metal-to-metal pulsed corona discharge to a dielectric-barrier discharge. The key difference is that in a barrier discharge processor, the barrier eliminates the problem of processor arcing. In the metal-to-metal type of processor, the arcing is controlled by the power supply's having very short, [*i.e.*, nanosecond] pulse widths. Creation of these very short pulses is straightforward but complicated and expensive.

Switching to a barrier-type processor simplified the power supply design. For either type of processor, a high voltage of ~20 to 30 kV was required. The average power was still driven by the energy density requirement for achieving a desired level of plasma oxidation. However, the pulse width now could be much larger, up to milliseconds, since the barrier prevents arcing. The proposed power supply would use a high-frequency transformer to generate the high voltage while minimizing the size. It would also use solid-state switches to create an alternating voltage to drive the transformer from a DC voltage.

Our baseline for full-flow testing of the Cummins B5.9 diesel engine generator set is based on a maximum flow of 9000 SLPM at 100% load on the engine and an engine-out NOx level of around 600 ppm. Figure 17 shows a contour plot of the NO-to-NO_2 oxidation efficiency in a plasma as a function of the specific energy density (in units of J/L per ppm of NOx) and C1/NOx ratio. To get 70% oxidation efficiency using a C1/NOx ratio of 4, the specific energy density required is about 0.06 J/L-ppm. For an engine-out NOx of 600 ppm, this translates into an energy density of 36 J/L. To accommodate the maximum flow of 9000 SLPM, the plasma processor must be capable of exciting the plasma with an average power of 5.4 kW. AGE diesel generators are nominally operated at less than 50% of the full load capacity. The exhaust flow rate would therefore be lower and we expected that 3 kW average power input to the plasma processor would be sufficient.

The volume of the active plasma region in the plasma processor in our full-flow test stand was around 1.5 L (2.5 inches in diameter and 18 inches long). Initially we had trouble coupling 3 kW of power into this volume using an AC power supply. This problem was fixed and we were able to deliver up to 3 kW of power to the plasma. We had made various modifications to both the plasma processor and the power supply design so that we could deliver a high average power at the lowest possible voltage while simultaneously keeping the plasma processor volume to a minimum.

Figure 25 shows the oxidation and reduction efficiencies in the full-flow plasma processor at power input levels of 0, 1, 2 and 3 kW. The HC additive used in this test was kerosene, with a C1/NOx of 4. The engine load was 35 kW, with an exhaust flow of 3200 SLPM and engine-out NOx of 500 ppm. The catalyst temperature was 260 C.

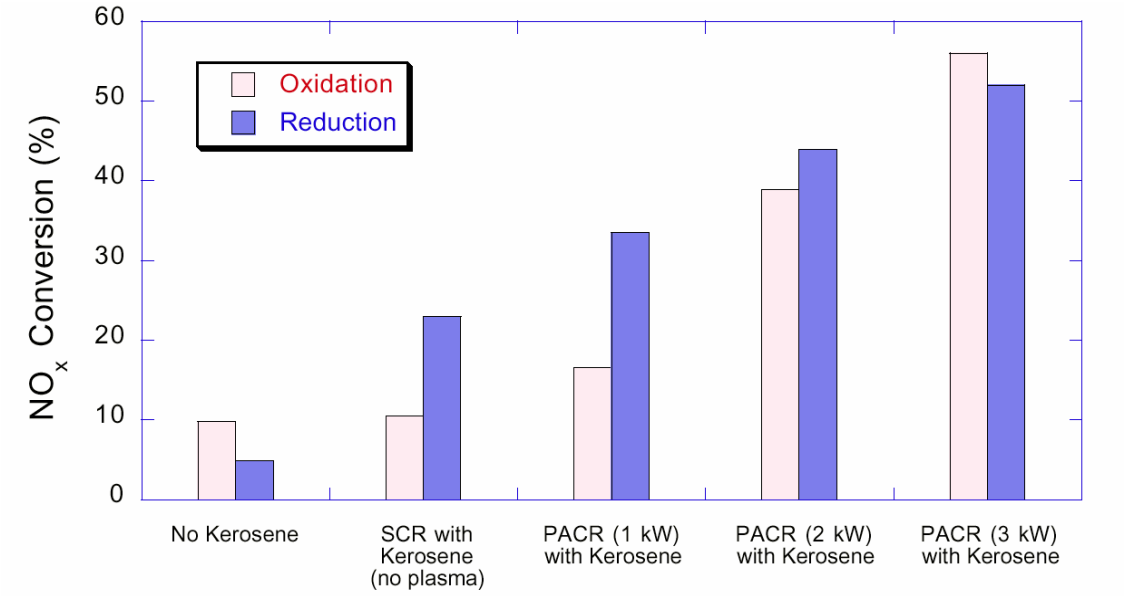

Figure 25. Oxidation and reduction efficiencies in the full-flow plasma processor.

During the long-duration testing of the full-flow plasma processor, the power supply transformer failed. This led us to a rather extensive investigation to understand the failure mode and the requirements for a replacement transformer.

Upon inspection of the waveforms for current and voltage that were recorded near the time of the failure, it became obvious why the transformer failed. The resonant configuration that we chose to use allowed us to reach the greater than 20 kV required to create the plasma. Unfortunately, the large capacitance used to create the resonant condition resulted in a large circulating current that grossly exceeded the transformer's rating.

There were two approaches to correcting this situation. The first path was to use a transformer with a much higher voltage rating so that resonance would not be required. The second path is to use the same transformer design that failed but at current values within its rating.

Using a higher-voltage transformer was successful at creating the plasma but also drew excessive current since the point design for the transformer did not match well to actual operating conditions.

To understand the problem, one needed first to understand how transformers are designed and rated. Each transformer has a power rating as well as voltage and current ratings. The power, voltage, and current match at one point. Exceeding any of these three parameters can result in failure. We purchased two transformer designs. The first was rated 3.5 kVa,

10 kV and the second was rated 4 kVa, 30 kV. The current ratings could be found by dividing the power (in kVa) by the voltage. Note the voltage ratings are RMS (root mean squared) values.

The 10-kV transformer was purchased as an off-the-shelf item. The 30-kV transformer was purchased as a custom design. We chose the 30-kV rating based on our experience at the time with a wire-in-cylinder geometry. When the-10 kV transformer arrived first we attempted to use it. Per conversations with the vendor, we decided to use it in a resonant mode. We tested it first with a lumped element capacitor and resistor load. This allowed us to reach the high voltage we thought was required. We then connected it to our real load; in this case we choose to make the cable long, about 100 feet, to achieve a distributed capacitance that was about the same value as our test off-line. The processor worked very well in this configuration until the failure.

Once we understood that the capacitive current was causing excessively large currents, we looked for ways to reduce it. The goal was to reduce the capacitance as much as possible but still operate near resonance to get the voltage boost needed to create the plasma. We shortened the cable as much as possible to about 25 ft, to cut the capacitive current by a factor of four. We did not know if we could then still achieve the voltage boost required. Likewise, we did not know if the current would be reduced sufficiently.

During our testing, the approach we took was to operate near resonance but not at full resonance. The goal was to find the minimum frequency at which we could deliver maximum power to the plasma processor, subject to the following restrictions:

- 3 kW maximum input power limit
- 500 mA peak current limit on the secondary

A further restriction was the transformer case temperature, but this restriction did not limit short-term testing of the power supply at its electrical limits. Tests were conducted at two input gas temperatures, 300°C and 200°C. The higher temperature was expected to cause the plasma to be more easily started and sustained, while the lower temperature limit would be a more-useful temperature operating point for the end user.

300 C run -- The plasma was initiated by operating at 1.8 kHz and increasing the pulse width until ignition. Then, the frequency was reduced and the pulse width simultaneously increased until the setting was at maximum. Finally, the frequency was adjusted with the pulse width knob maintained at the maximum value until 10 amps of current were drawn in the primary. The frequency setting was a function of the temperature in the FFP, which caused more or less power to be dissipated; they were coupled together. Figure 26 shows the DC current in the power supply as a function of frequency.

At about 1.6 kHz, the current started to increase quickly and this was accompanied by rapid heating in the plasma/catalyst system. Ultimately, the catalyst temperature was 50°C above the inlet gas temperature of 300°. Figure 27 shows some other miscellaneous trends with increasing frequency. The oxidation level was quite high at maximum power dissipation. The case temperature started to climb and went to a value as high as 59°C before the test was terminated to start another test.

At 1724 Hz, the maximum secondary voltage was 23.6 kV and the peak current was about 480 mA, slightly below the 500-mA maximum based on the kVa rating of the transformer. Figure 28 shows the I–V plot of the secondary at this point. Diagnostics on the secondary suggested that the power dissipation into the plasma processor was 3.4 kW.

200 C run -- A similar test to that described above was run with the input gas temperature at 200°C. The plasma was ignited at high frequency, the frequency was lowered with concomitant increase in the pulse width, then the frequency was adjusted until the primary drew 10 amps. Figure 29 plots the change in frequency versus elapsed time. At approximately 1.85 kHz, the plasma was stably drawing 10 amps into the primary and dissipating the maximum power into the load in the secondary. The pulse width knob was at maximum.

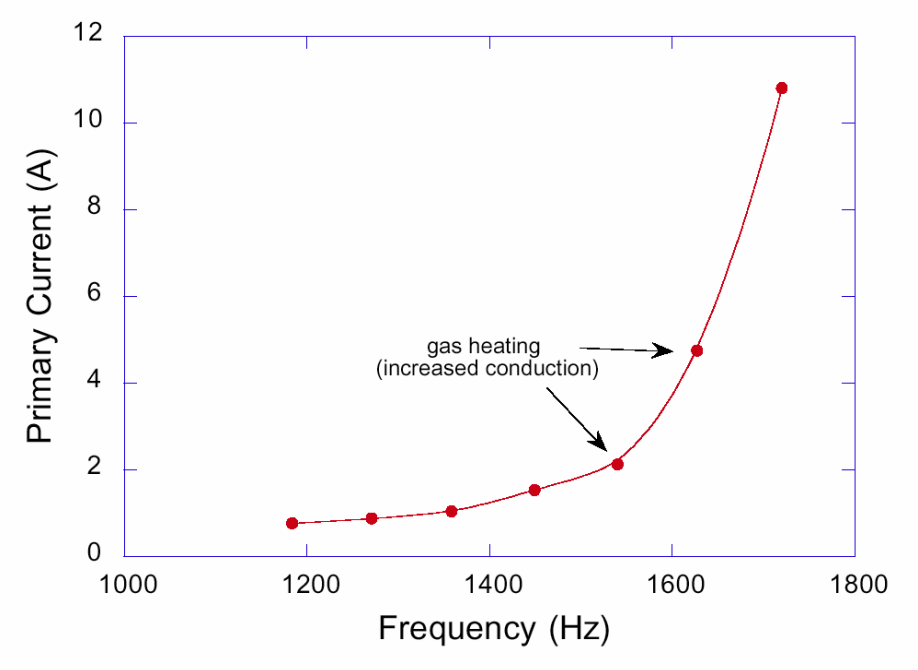

Figure 26. DC current in the power supply as a function of frequency. 10-kV transformer, 35 kW engine load, 300 C gas temperature in plasma processor, 3000 SLPM flow, C1/NOx of 6.

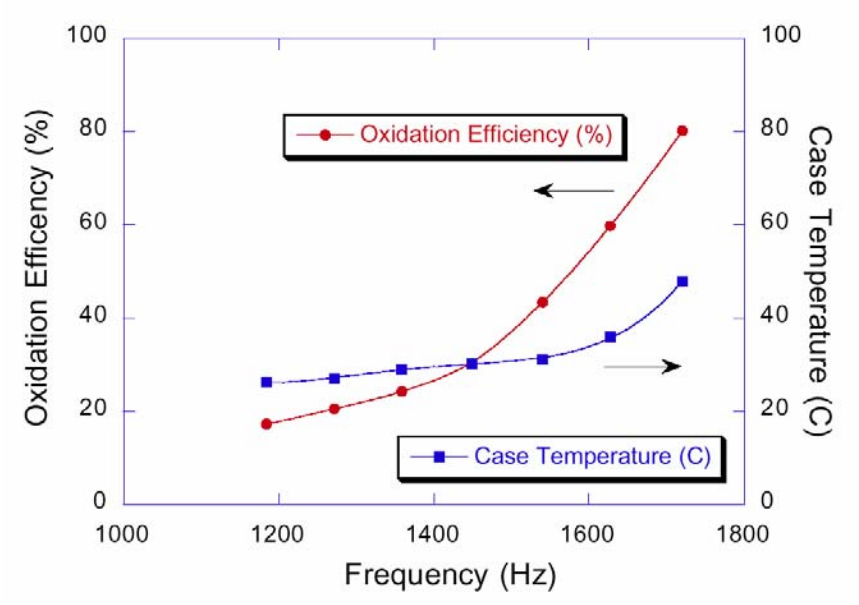

Figure 27. Oxidation level and transformer case temperature during the frequency optimization process.

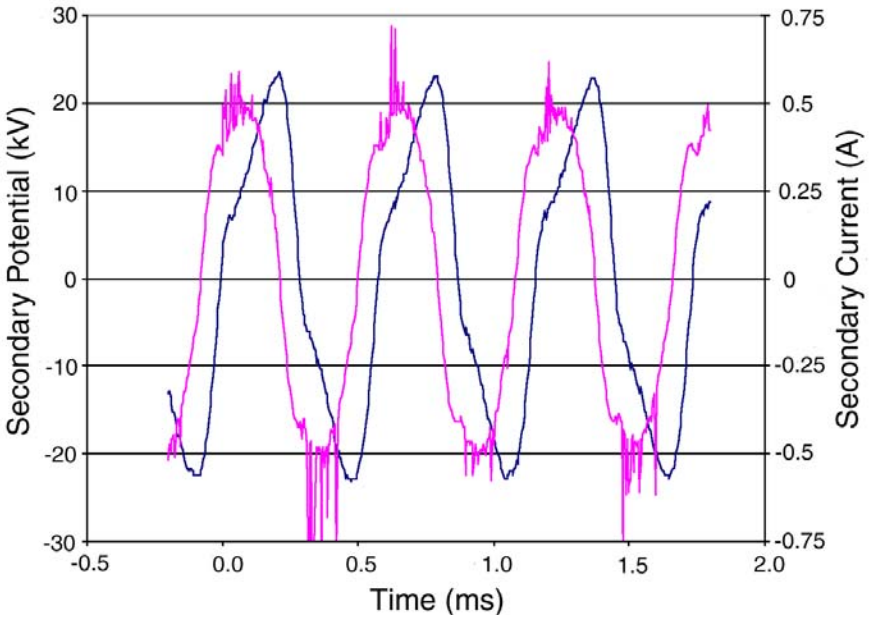

Figure 28. Voltage and current on the secondary while running at 1724 Hz.

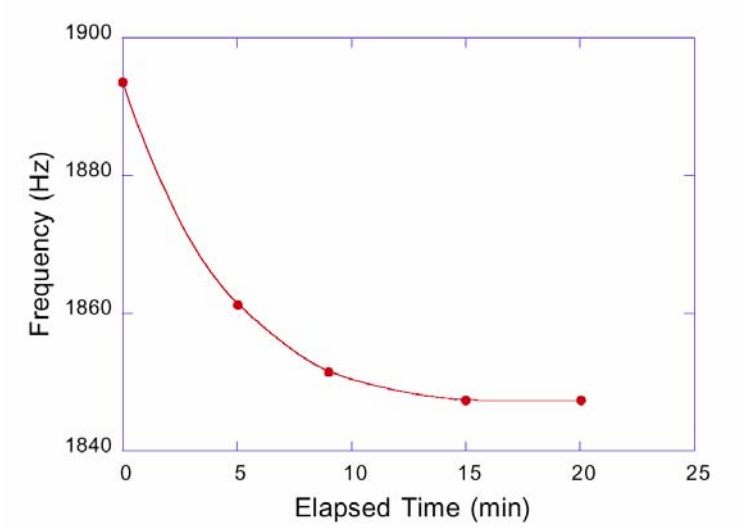

Figure 29. Reduction in the voltage frequency over time as the plasma processor system comes to thermal equilibrium.

Figure 30 shows the I–V behavior of the secondary under these conditions. The peak voltage was 22.4 kV and the peak current was ~400 mA, well below the 500-mA limiting value. The diagnostics on the secondary suggested that power dissipation in the plasma processor was 3.1 kW.

Figure 31 plots the rise in the case temperature during the course of this test. Note that the cooling fans were running during this test, blowing air around the transformer. It had previously been determined that the fans could lower the case temperature by 10–20°C. Clearly, the operating temperature will be exceeded quite soon even with a more-active cooling system and limiting the bulk of the transformer loss to core losses.

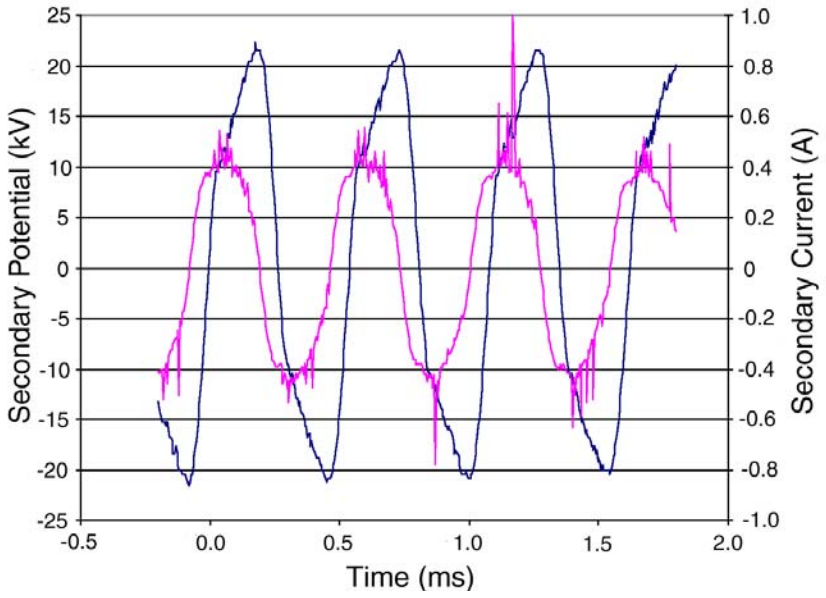

Figure 30. Voltage and current on the secondary for the 200 C run under stable operating conditions.

Testing indicated that we could stay within the transformer ratings except perhaps at the maximum temperature. We recommend performing additional testing while providing additional cooling to the transformer. The cooling may be supplied by additional fans or possibly a water-cooled plate.

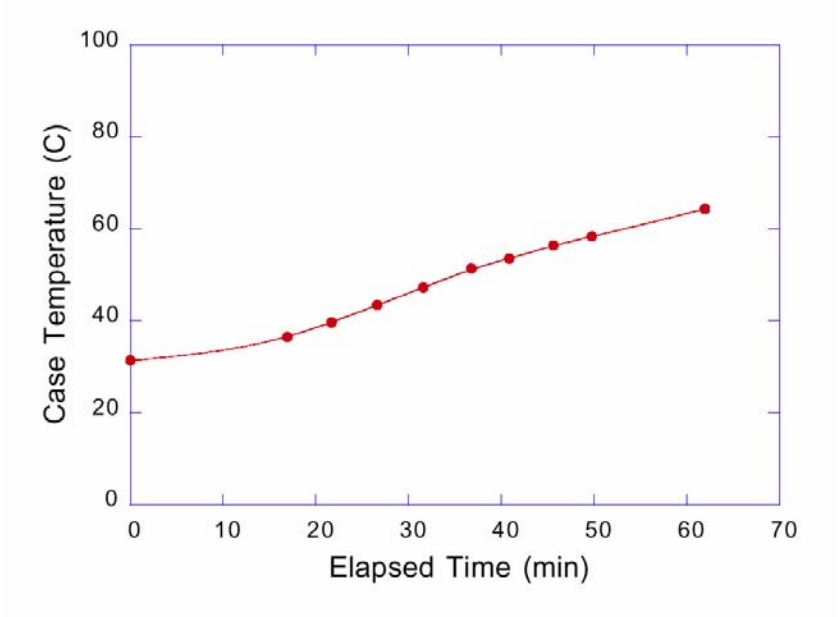

Figure 31. Transformer case temperature vs time during the 200 C test.

Eventual suitability of the 10-kV transformer will largely be determined by whether or not one can adequately cool the transformer. The alternative would be a new transformer rated higher in voltage, for example, ~15 kV, that could be operated with a very short cable.

Milestone 12: Transfer and Setup of Air Force Diesel Generator. Status: Completed.

Generator Transfer from AFRL to LLNL

The transfer of an A/M32A-86A diesel generator set from AFRL to LLNL was a challenge of some duration that became a major source of delay in the project. Lt. Col. LeAnn Brasure, AFRL Commander's Representative to LLNL, helped greatly in facilitating this transfer. The genset was finally picked up from McClellan AFB in Sacramento and delivered to LLNL 28 June 2000.

Mechanical Modifications

The Air Force genset (model A/M32A-86A, Figure 32) was received and the operations manual reviewed by operating personnel to ensure safe operation of the unit. The generator was placed onto our test facility pad and secured in the event of an earthquake. Initial questions about fueling the generator were satisfactorily resolved by McClellan personnel. We had a concern that the use of fuels other than JP-8, the standard fuel used to operate the engine, would be detrimental to the generator performance. However, we were told that we could use any fuel to operate the engine.

Figure 32. Identification plate of the A/M32A-86A generator set.

The first set of tests required careful characterization of the flow rate and temperature of the engine exhaust as a function of engine load. To meet this goal, an orifice gauge flow measuring device was installed in both the intake and exhaust lines of the engine. This served to cross-correlate the flow measurements at ambient and elevated temperatures and also gave insight into the effect of the supercharger on the engine. The A/M32A-86A generator is a two-stroke 72-kW diesel engine. Our experience had mostly been with a four-stroke 100-kW diesel engine from Cummins. We needed to characterize the A/M32A-86A engine operating conditions more carefully before we could design the emissions control system.

Thermocouples were installed at various points in the engine exhaust line to understand the temperature conditions that an inline catalyst would experience while treating the NOx in the exhaust. In addition, sample lines for NOx and HC diagnostics were extended to the genset for real-time performance monitoring.

Some minor additional safety features needed to be installed on the genset to comply with facility safety regulations. A key switch, keyed to the building roof, was installed to ensure that the facility roof couldn't be accessed when the genset was operating.

LLNL's Air Quality District had shortly before stricken the air permit exemption for research engines. This meant that we would need to get an air permit to continue operating this equipment. At the time, we were operating under a "Loss of Exemption" variance, but that temporary condition was no longer available to us. At the end of the project, our Environmental Protection Department was negotiating a time limit of operations with the Air District, and we had already been informed that 100 hours per month was considered an excessive level of usage.

An initial design of a catalyst holder to fit onto the genset was completed. Some prototype parts were fabricated to understand some of the manufacturability issues in the design. We made the catalyst system as compact as possible consistent with good deNOx performance.

Load Bank Modifications

The load bank was originally designed to draw its control power from the genset as well as provide loading to dissipate engine power. One cannot operate in this mode with the Air Force generator because of the difference in supply voltage. Therefore, the load bank required modification to operate the control systems on external 480-V, 3-phase AC. Furthermore, modifications were required to incorporate the safety features designed into the genset. Specifically, the generator uses 24 V supplied by the load to energize the main contactor. The load bank was modified to supply this voltage and it served as a safety feature—if the power cord were severed in any way during operation, the generator would stop supplying power.

The load bank was originally designed to dissipate 125 kW at 480 VAC, 60 Hz. The Air Force generator is rated at 72 kW at 200 VAC, 400 Hz. We had two choices in modifying the load bank to properly dissipate the genset energy. One option was to divide the resistance in half and use only half the available load resistors. That relatively simple change in configuration would allow us to operate the genset more quickly, but limit us to a computed power dissipation of only 45 kW. The key limitation was the current-handling capability of the contactors, wiring and fuses in the power-dissipation circuit. The second option was to reconfigure the load bank with components that could handle the higher currents needed to achieve a full-load condition. We started to implement this upgrade; the high-current contactors were installed and the resistance division was completed.

Operation at partial load was justifiable since the genset typically operates at loads well below the maximum value. We were able obtain valuable design information at reduced load and extrapolate to higher loads to facilitate the deNOx process design. However, the overall operation of the system may require some operation at higher loads, so it would be necessary that the system would perform as anticipated, if it became necessary.

At end of project, we were designing and installing additional diagnostics on the system to indicate the actual power dissipated in the load. This consisted of a shunt to be placed in series with one phase of the load bank input. Each phase leg was to have been tested for consistency, after which one leg was to have been chosen to serve as the diagnostic for total power dissipation.

We tested the upgraded contactor components to ensure that they would function normally when the genset power was applied. All components were checked and the installation went without any failures, but system tests had not been accomplished.

Figure 33 shows the A/M32A-86A generator set with the load bank on the right. Figure 34 shows a closer view of the engine of the A/M32A-86A generator set, and Figure 35 shows a closer view of the control panel of the load bank used with the generator set.

Figure 33. The A/M32A-86A generator set with the load bank on the right.

Figure 34. Engine of the A/M32A-86A generator set

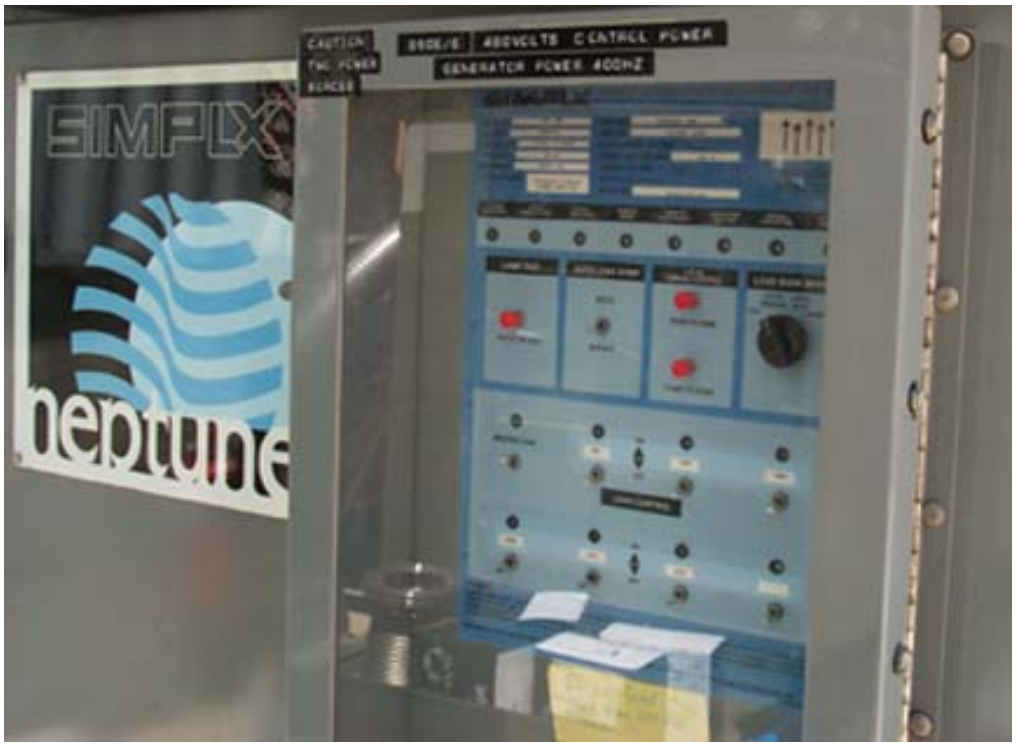

Figure 35. Control panel of the load bank used with the generator set.

Figure 36 shows the range of exhaust temperatures for four-stroke and two-stroke diesel engines. The A/M32A-86A generator is a two-stroke diesel engine and it is typically operated by the Air Force at only 25 percent of full load capacity. Most of our data have

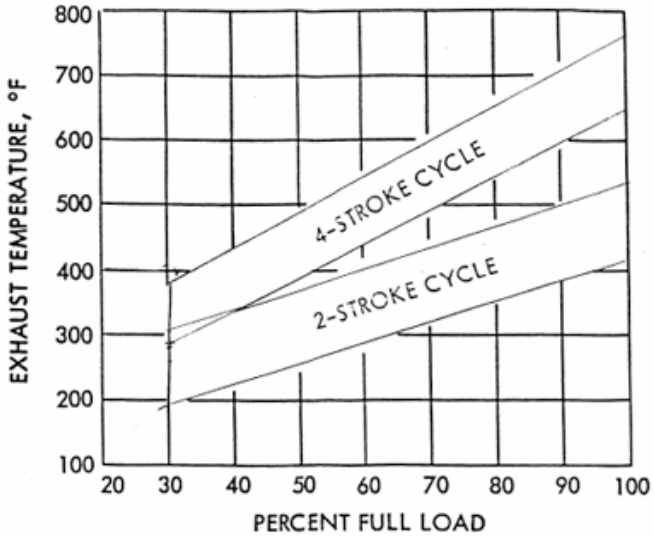

Figure 36. Range of exhaust temperatures for four-stroke cycle and two-stroke cycle diesel engines. The A/M32A-86A generator, which is a two-stroke cycle diesel engine, is typically operated at only 25 percent of full load capacity.

been taken using a four-stroke cycle Cummins diesel engine, operating at above 50 percent (often at 80 to 100 percent) of full load capacity. The exhaust temperatures in the Cummins engine tests are much higher than what we expect to get from the A/M32A-86A generator. At 25 percent of full load, the A/M32A-86A

engine will have exhaust temperatures of 300 F (150 C) or less, according to Figure 6. None of the best available NOx or soot catalysts can operate effectively at these low temperatures. The catalysts will have to be thermally assisted, electrically assisted or plasma-assisted. Our measurements of the exhaust temperature and flow rate will provide us essential information on the needs of the emissions control system. We suspect that the low exhaust temperature of the A/M32A-86A generator will highlight the benefit of plasma-based emissions control systems over conventional catalytic techniques.

Milestone 13: Simultaneous treatment of NOx and soot. Status: Completed.

During field operations, the A/M32A-86 diesel generator is nominally operated at 25% or less of the full load capacity. This operation has two major consequences: (a) it causes the buildup of unburned diesel fuel and carbon residues in the exhaust system, and (b) the exhaust temperature is too cold for the soot catalyst to function effectively.

Soot (carbon residues) was a serious cause of failure in the high-voltage insulators of the plasma processor that was used for NOx control.

We therefore engaged in the study of how to use the plasma for controlling the soot in the exhaust. The technique for controlling soot is based on our observation of what happened to the plasma processor. We noticed the absence of soot accumulation on surfaces that were directly exposed to the plasma, as shown in Figure 37.

We hypothesized that the same plasma can deal with both the NOx and the carbonaceous particulates, shown in Figure 38. The plasma streamer has a non-thermal component that

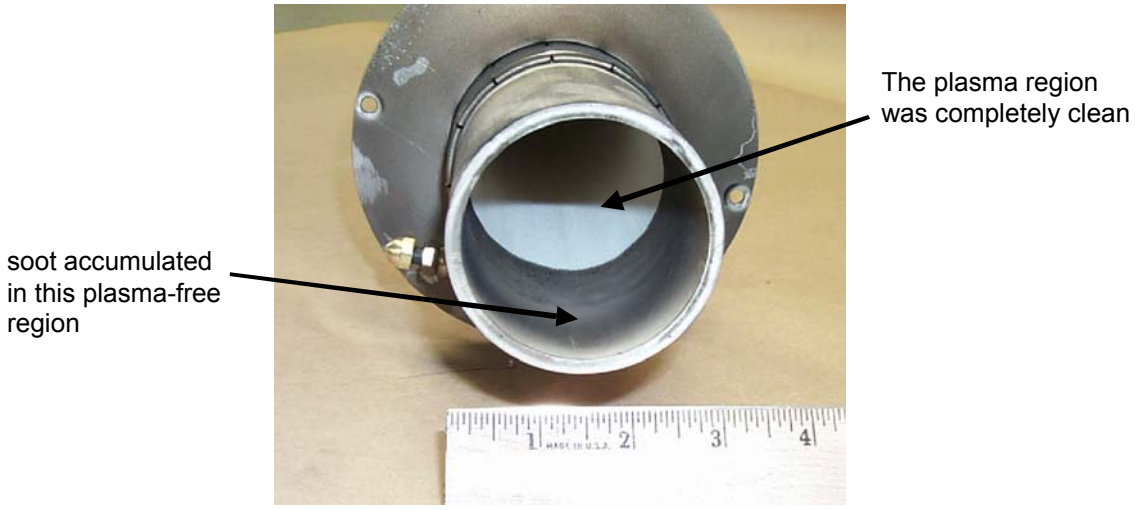

Figure 37. Picture of the inside surface of the plasma processor showing the absence of soot accumulation in the region directly exposed to the plasma.

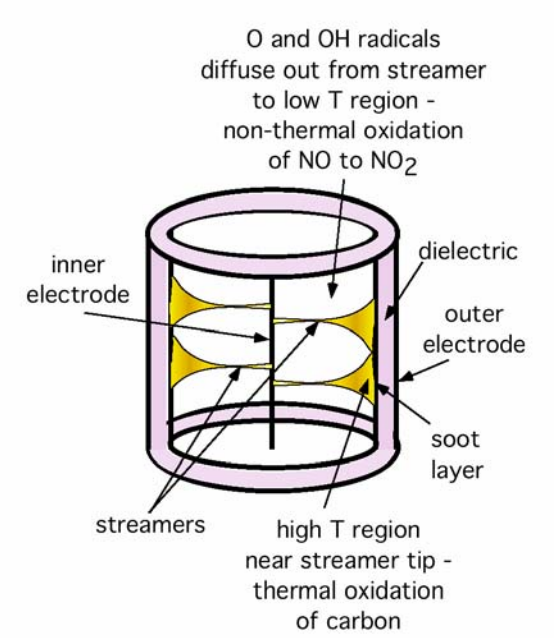

Figure 38. Hypothesis of how the plasma can simultaneously oxidize NO and soot.

is responsible for the oxidation of NO to NO_2. At the tip of the streamers, a thermal component is responsible for the thermal oxidation of any carbonaceous particulate that has been electrostatically collected. Figure 39 shows the concept for simultaneous control of NOx and carbonaceous particles, using particle trapping by electrostatic precipitation.

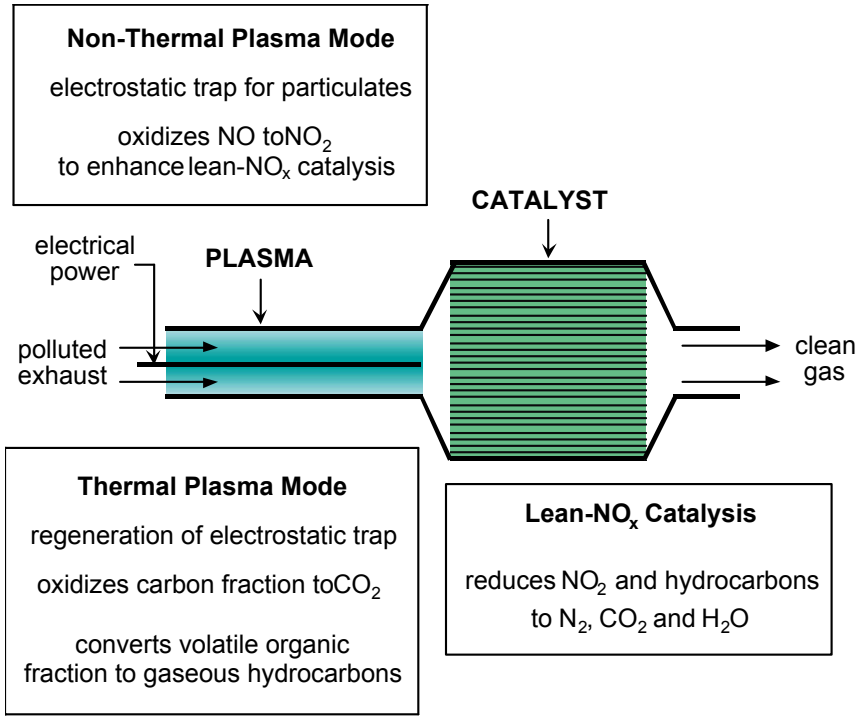

Figure 39. Simultaneous control of NOx and carbonaceous particles, using particle trapping by electrostatic precipitation.

Our first concept was based on using electrostatic precipitation to trap the particles. However, we decided to switch to a Corning wall-flow filter to enhance the particle-trapping efficiency. The Corning wall-flow filter is known to have a very high particle-trapping efficiency (> 90%). We took a commercially available Corning wall-flow monolith and cut pieces of wafers for our tests, as shown in Figures 40 and 41. The plasma-regenerated particulate filter used in our bench-scale test is shown in Figure 42.

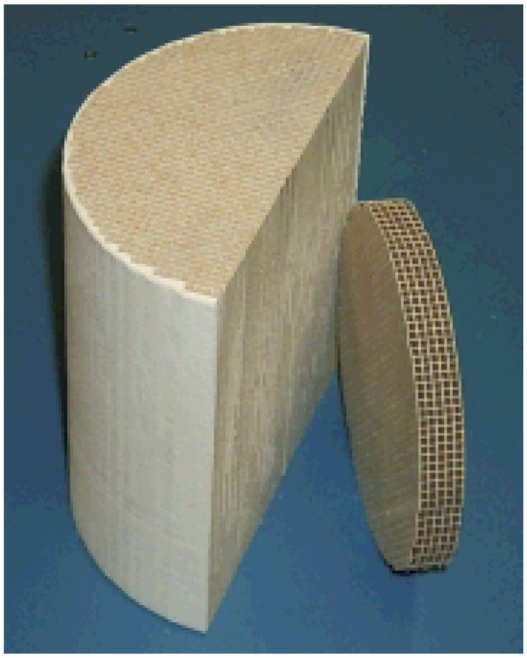

Figure 40. Picture of a wafer filter (right) cut from a Corning wall flow monolith (left).

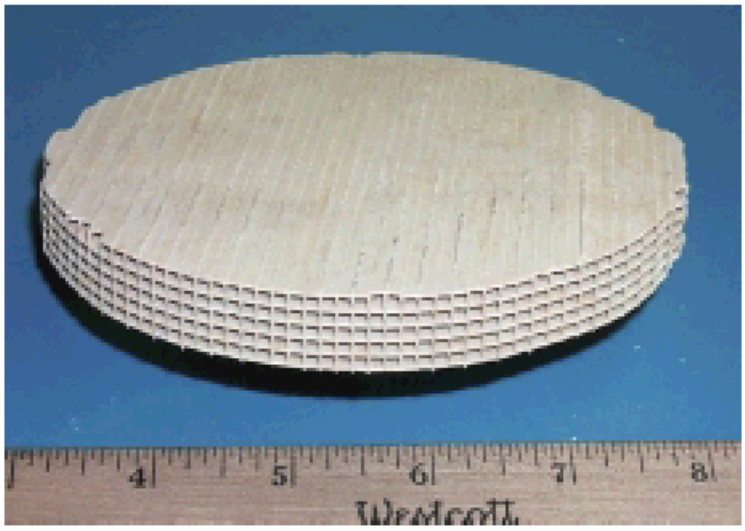

Figure 41. Picture of a wafer filter.

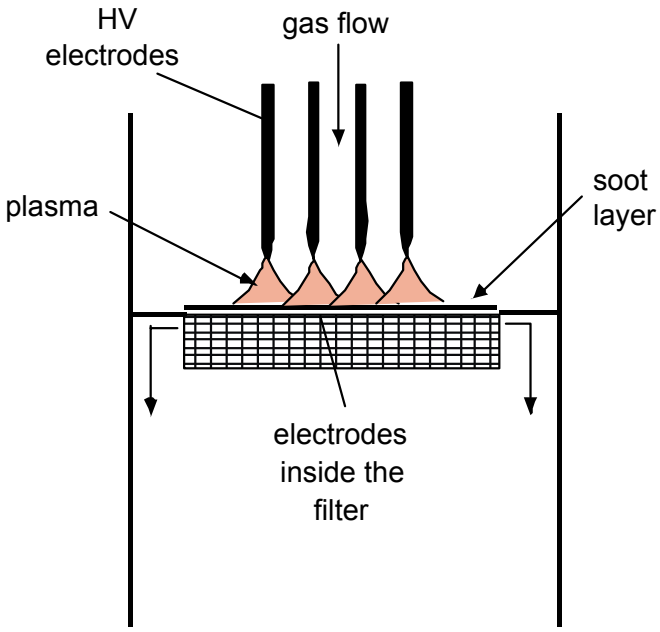

Figure 42. Plasma-regenerated particle filter using a wafer cut from a Corning wall-flow monolith.

We performed bench-scale tests to demonstrate the feasibility of the plasma-regenerated particle filter shown in Figure 42. We characterized the products of particle oxidation. We measured the specific energy density (electrical energy per mass of particulate) for particle oxidation. Based on the specific energy density we analyzed power consumption for full-scale application to a heavy-duty diesel engine. We also determined whether the electrical power consumption in the plasma for plasma-assisted catalytic reduction of NOx was compatible with that required for plasma regeneration of the particle filter.

Figure 43 shows an FTIR spectrum of the products of the plasma thermal oxidation of the soot layer collected on the Corning wafer. Direct exposure of the soot layer to the plasma

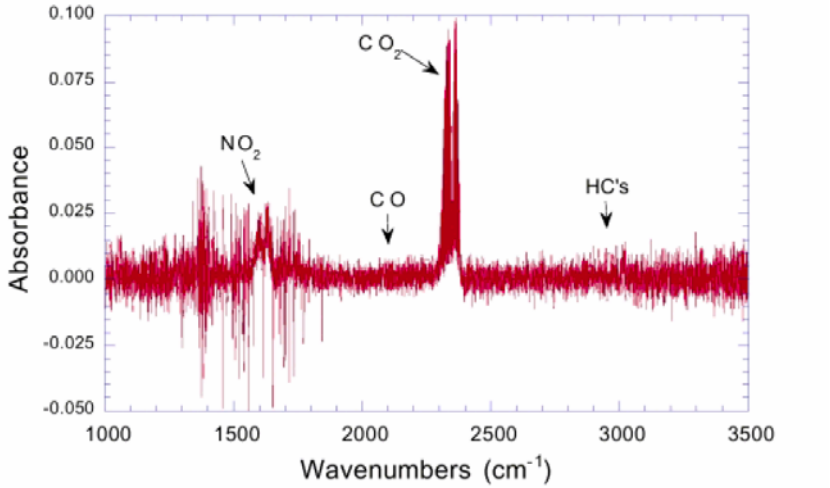

Figure 43. FTIR spectrum of the products of the plasma oxidation of the soot layer collected on the Corning wafer.

resulted in complete oxidation to CO_2. The specific energy for carbon oxidation was measured as 2.5 J of electrical energy per microgram of carbon. This specific energy density could be used to determine whether the electrical power consumption in the plasma for plasma-assisted catalytic reduction of NOx is compatible with that required for plasma regeneration of the particulate filter.

Suppose we wanted 70% efficiency for NO-to-NO_2 oxidation in the plasma. Consulting Figure 17, this could be achieved using a specific energy density of 20 kJ/g(NOx) and C1/NOx of 6. For a heavy-duty diesel engine with an exhaust flow of 9000 standard liters per minute (slpm) containing 500 ppm of NOx, the NOx emission rate is 500 g(NOx)/hr. The electrical power required would therefore be 500 g(NOx)/hr multiplied by 20 kJ/g(NOx). This is equal to 3 kilowatts.

Our measured specific energy for carbon oxidation was 2.5 J per microgram of carbon. The amount of carbon we could oxidize by the same 3-kW plasma was therefore 4.3 g(carbon)/hr. Suppose the carbon emission rate were 0.1 g(carbon)/kW-hr. A 100-kW engine would emit 10 g(carbon)/hr. Assuming the particulate filter traps all the carbon, the filter regeneration efficiency by the plasma is 43%.

We needed to improve the efficiency for carbon oxidation to 1 J/μg of carbon to completely regenerate a particulate filter for an engine whose particulate emission rate is 0.1 g(carbon)/kW-hr. We believe this goal can be met by the right choice of electrode gap spacing. At project's end, we were working on a scaled-up design to demonstrate a plasma-regenerated particle trap that would be compatible with the plasma-assisted catalytic reduction of NOx.

Milestone 14: Pilot facility and emissions characterization. Status: completed.

An A/M32A-86A diesel generator set was transferred from McClellan AFB in Sacramento to Lawrence Livermore National Laboratory. The generator was placed onto our test facility pad, secured, and connected to a load bank. Figure 44 shows a picture of this diesel generator, with the emissions control system attached close to the engine. The current location of the emissions control system was chosen for convenience in assembling and disassembling for various experiments. There is ample room in the cart under the engine for a relatively large emissions control system, if such is required to achieve high removal rates for NOx and particulates.

Thermocouples were installed at various points in the engine exhaust line to understand the temperature conditions that will be experienced by an inline catalyst to treat the NOx and/or particles in the exhaust. In addition, sample lines for NOx and HC diagnostics were extended to the genset for real-time performance monitoring.

Measurements of the exhaust temperature of the A/M32A-86A diesel generator set are shown in Figure 45 as a function of engine load. The A/M32A-86A generator is a two-stroke cycle diesel engine and it is typically operated by the Air Force at only 25 percent of full-load capacity. Our measurements show that the exhaust temperature at 25-percent

Figure 44. The A/M32A-86A diesel generator set with the emissions control system attached close to the engine.

engine load is only about 200 C. None of the best available NOx or soot catalysts can operate effectively at these low temperatures. The catalysts will have to be thermally assisted, electrically assisted or plasma-assisted.

Measurements of the NO_x concentration in the exhaust of the A/M32A-86A diesel generator set are shown in Figure 46 as a function of engine load. About 500 ppm NO_x is emitted when the engine load is 25 percent. NO_x emission is very high at higher engine loads.

We consider load control to be a significant factor in managing the performance of any pollution abatement strategy, since it also addresses the wet-stacking problem. Therefore, intelligent load management could be used to broaden the design space of any pollution abatement scheme. As such, we cannot rule out the use of a precious-metal-based soot-control method, since that technology is readily available and well understood.

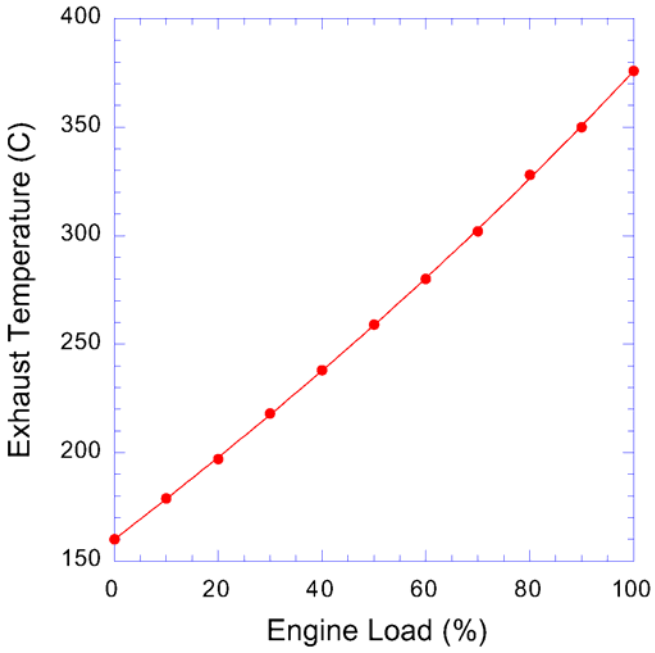

Figure 45. Exhaust temperature of an A/M32A-86A diesel generator set vs engine load.

One concept we attempted actually used a form of wet stacking to advantage to maximize the trapping efficiency of a carbon oxidation system. A metal-foil-based HC catalyst on the market is purported to be a very efficient HC oxidation catalyst. Its efficiency stems in part from an internal design that provides for turbulent flow locally within the catalyst

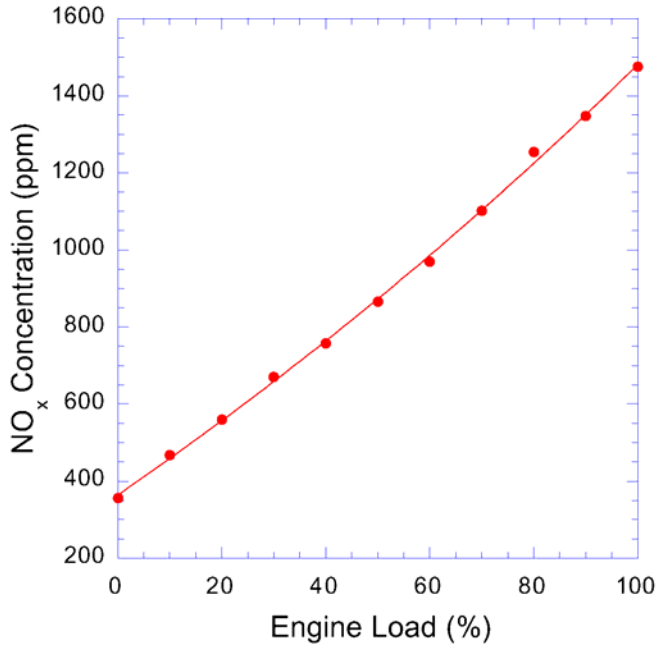

Figure 46. NO_x concentration in the exhaust of an A/M32A-86A diesel generator set vs engine load.

structure. Contact with the catalytic surfaces was enhanced and the oxidation was more efficient. Based on this monolith design, a simple concept for soot trapping and oxidation could be devised.

When the exhaust temperature is low, we might increase the soot trapping efficiency of the oxidation catalyst by injecting some diesel fuel onto the catalytic surfaces. HC adhering to the monolith might increase the soot trapping efficiency because of the turbulent flow within the structure. Thus, an oxidation catalyst might act as a soot trap for a reasonable period of time. When the catalyst is "loaded," it might be regenerated by simply by increasing engine load to raise the exhaust temperature. At catalyst light-off, the trapped carbonaceous soot would be cleanly oxidized away, along with the HC coating. Then, the process would be repeated.

Injection of HC fuel would be required for implementation of any plasma-based NOx-control technology. Volatile HCs greatly increase the oxidation efficiency of the plasma to form NO_2 from NO. Thus, injection of HC didn't need to be avoided if the HC could perform one or more beneficial functions.

Electrostatic pellet bed: It is possible to construct a pellet bed that acts both as a particulate trap and as an HC- and soot-destruction bed via use of a plasma. In addition, with attention to the requirements for a plasma-based NOx-control scheme, plasma could be applied to solve both the soot and NOx problems simultaneously. However, considerations of the plasma power supply to be used made it imperative that we understand what the requirements were for the pellet materials and how they would behave under an anticipated load cycle.

Barium titanate is a high-dielectric material that was a good candidate for the pellet material. One needs a high-dielectric material to exclude electric fields from the ceramic and cause corresponding compression of the field lines within the gas interstices. This, in turn, would cause plasma breakdown to occur within the interstices and would allow for power dissipation to occur where particulate matter was being trapped.

The first requirement for understanding how such a device might work was to consider how the dielectrics in a pellet bed arrange themselves and to find out what the average dielectric constant in the bed would be. There were two limiting possibilities, which are described in Figure 47.

In this case, the high-dielectric-constant barium titanate pellets represents C_1 and the ambient air represents C_2. Measurements of the pellet bed overall dielectric constant resulted in a value of approximately 5, indicating that the series-equivalent circuit is the better model of the electrical characteristics of the pellet bed. This was an advantageous outcome because it indicated that significant power dissipation by the plasma can occur within the pellet bed and it also suggested that temperature effects on the average dielectric constant will be small and not contribute to changes in the power-dissipation levels. At project's end, we were in the process of verifying this fact experimentally with a small-scale pellet bed in a laboratory oven.

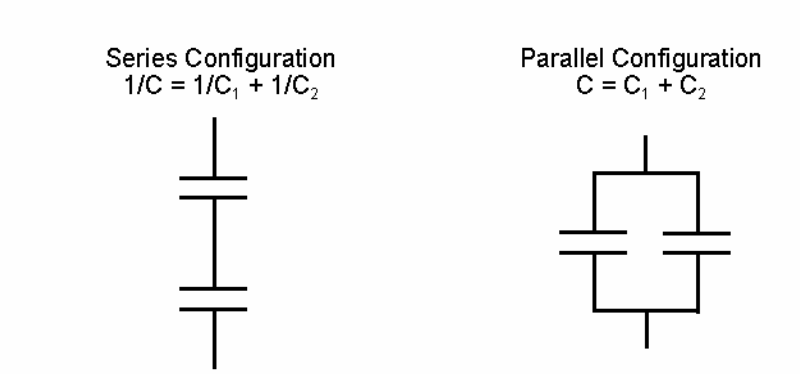

Figure 47. Limiting case of series- or parallel-equivalent circuit for high-dielectric-constant pellets in a bed configuration.

Bag filter with plasma regeneration: Lower temperatures anticipated in the AGE gensets opened up the possibility of utilizing alternative filtering media for soot collection and destruction. Bag filters could be used to collect soot from engines, as they have a number of adjustable parameters, such as type of weave and flexibility in designing sizes and shapes. Also, bag filters that withstand higher operating temperatures are in commercial production, with some filtration media able to withstand temperatures as high as 500°C. Bag filtration is simple and cost effective to deploy. The key to implementing such a scheme is the ability to regenerate the bag by application of a plasma.

Typically, bag filters are regenerated by reverse flushing with gas, usually coupled with some sort of mechanical agitation. We investigated the possibility of regenerating a bag-filter membrane with a plasma discharge. A test system using bag material from Standard Filter Corporation was built and used in the manner illustrated in Figure 48.

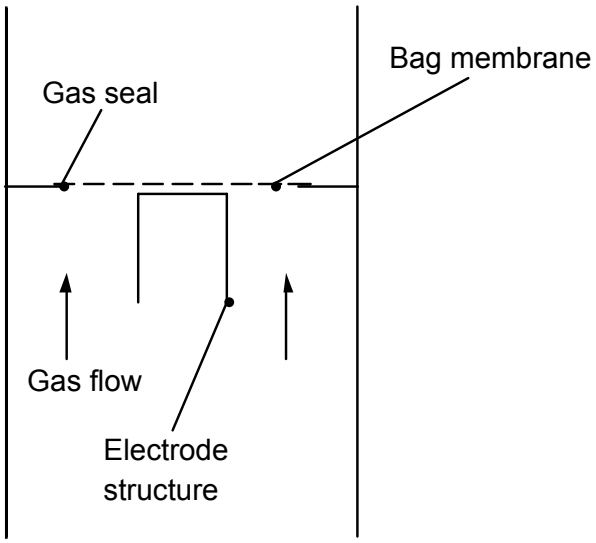

Figure 48. Schematic diagram of the bag-filter membrane plasma-regeneration test.

The bag membrane was fitted to collect soot from the diesel engine in an offline step, then put into the test system shown in Figure 48. In this system, a controlled flow of bottled gases was delivered through the bag while plasma discharges were developed on the electrode structure. The temperature of the system was also controlled to match anticipated engine exhaust temperatures. Our emphasis was to find out under what conditions we could clear the bag material of carbonaceous soot. By adding a downstream Fourier Transform Infrared (FTIR) spectrometer, we were able to characterize the level of carbon removal as well as determine the species liberated by the process. With knowledge of the plasma power, we were then able to obtain some measure of the energy required to perform the regeneration process.

Figure 49 shows an FTIR spectrum of the effluent of one of the filter regeneration tests. Plasma regeneration of trapped soot particles results only in the formation of CO_2. No evidence of CO or the release of trapped HCs is apparent.

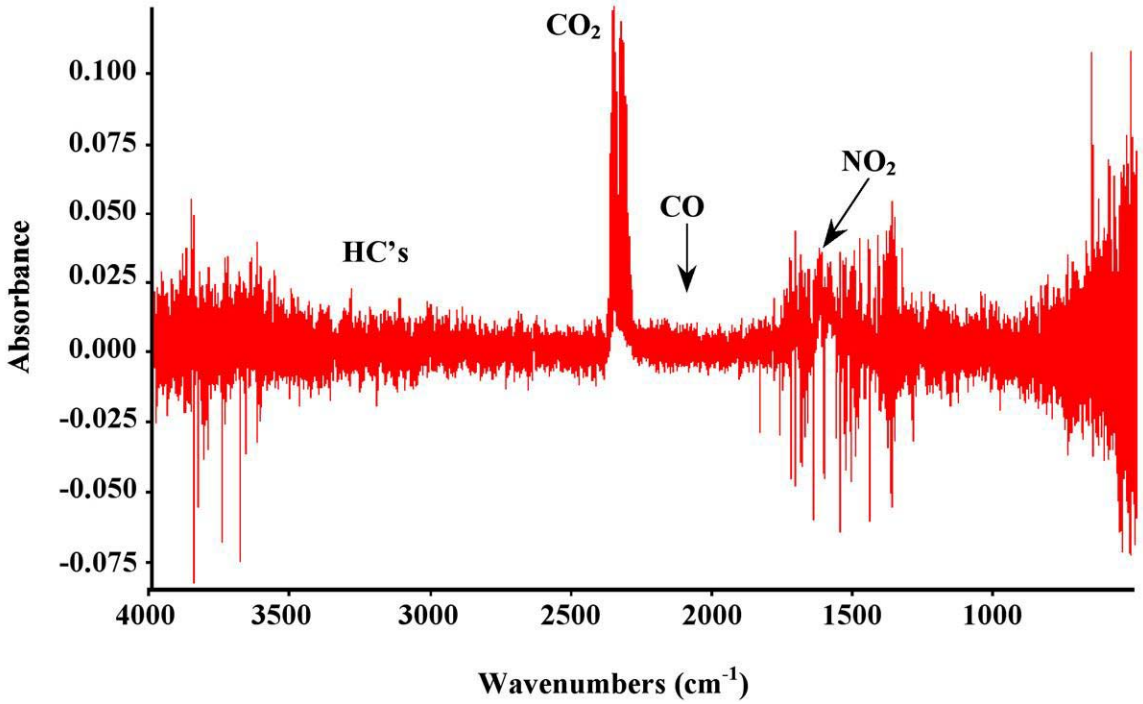

Figure 49. FTIR spectrum of the gaseous effluent from a filter regeneration experiment. The background gas was 20% O_2 in N_2 and the gas temperature was 200 C.

Figure 50 shows the result of exposure of the bag filter material to the plasma, which show clearly that it is possible to remove soot from the bag filter material using a plasma discharge.

To establish the efficiency of the process, it was necessary to determine the efficiency of carbon removal. In our laboratory, we found it convenient to express this in units of mass carbon removed per unit of energy. Since the FTIR showed that carbon was removed

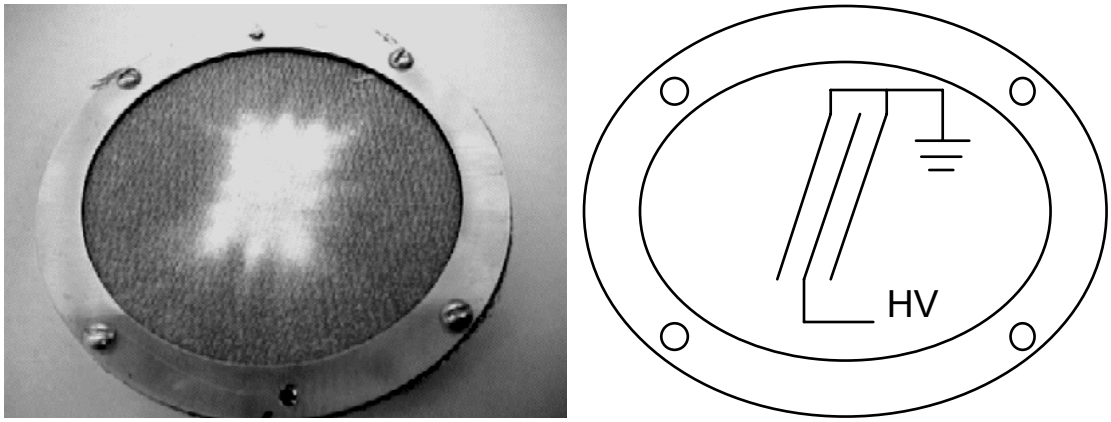

Figure 50. Photo of the bag filter material after exposure to plasma. The diagram on the right illustrates an electrode configuration.

only as CO_2, we needed only to monitor the removal rate of carbon and the power dissipation in the plasma. Under a typical set of operating conditions, we found that the carbon removal rate was 0.4 μg C/J.

Given the soot measurements described above, we performed the following analysis. The genset had a flow rate of 12000 L/min, or 200 L/sec. Multiplying by the density of air (1.3 g/L) gave a standard mass flow of 260 g air/sec. The soot mass fraction emitted by the engine was ~1.6 x 10^{-6}, giving a soot mass flow rate of 4.16 x 10^{-4} g C/sec, or 416 mg C/sec. Given the carbon removal rate above, the power requirement to perform this function would be

$$\frac{416\mu gC\,\mathrm{sec}^{-1}}{0.4\mu gCJ^{-1}} = 1040J\,\mathrm{sec}^{-1} = 1.04kW$$

This power requirement is only 2% of the output of a generator operating at 50 kW, exclusive of consideration of the efficiencies of plasma generation. Also, we believe that the efficiency of this process could be improved substantially by continued attention to the design of the electrodes producing the plasma. Essentially, one must limit heating of the air, which wastes energy. Thus, a surface discharge mode was the preferred method of producing the plasma and coupling to the collected soot.

On-Board Load Management

Regardless of the design of the pollution-abatement equipment, active abatement will require the dissipation of additional energy. Fortunately, this will also help to counter the "wet stacking" problem. In addition to dissipating more energy to perform active pollution control, additional control of the genset load could be accomplished by installing an on-board load bank to increase the generator load when needed to raise the exhaust temperature or to condition parts of the aftertreatment system, when needed. An

example of a forced-convection-cooled load bank is shown in Figure 51. During this study, this unit was commercially available from Avtron.

Figure 51. A forced-convection-cooled load bank.

Such a device could be placed in front of the engine radiator for forced cooling from the engine fan. It was also possible to design a liquid-cooled system, which could be much more compact. Besides being compact, the liquid-cooled system could be made much safer because of its sealed construction. Finally, a load control system would have to be developed so that generator load could be smoothly transferred from the on-board load bank to the aircraft when high loads were required. When the generator load required at the aircraft is low, the control system could shift the generator load in a predetermined manner back to the on-board load bank.

U.S. Patents granted during the performance period of this project:

NOx Reduction System Utilizing Pulsed Hydrocarbon Injection.
U.S. Patent 6,202,407. March 20, 2001. R.M. Brusasco, B.M. Penetrante, G.E. Vogtlin, B.T. Merritt.

Nitrogen Oxide Removal Using Diesel Fuel and a Catalyst.
U.S. Patent 6,119,451. Sep. 19, 2000. G.E. Vogtlin, D.A. Goerz, M.C. Hsiao, B.T. Merritt, B.M. Penetrante, J.G. Reynolds.

Plasma Regenerated Particulate Trap and NOx Reduction System.
U.S. Patent No. 6,038,854. March 21, 2000. B.M. Penetrante, G.E. Vogtlin, B.T. Merritt, R.M. Brusasco.

Plasma-Assisted Catalytic Storage Reduction System.
U.S. Patent No. 6,038,853. March 21, 2000. B.M. Penetrante, G.E. Vogtlin, B.T. Merritt, R.M. Brusasco

Catalytic Reduction System for Oxygen-Rich Exhaust.

U.S. Patent Number 5,893,267. April 13, 1999. G.E. Vogtlin, B.T. Merritt, M.C. Hsiao, P.H. Wallman, B.M. Penetrante.

Pre-Converted Nitric Oxide Gas in Catalytic Reduction System.
U.S. Patent Number 5,891,409. April 6, 1999. M.C. Hsiao, B.T. Merritt, B.M. Penetrante, G.E. Vogtlin.

Plasma-Assisted Catalytic Reduction System.
U.S. Patent No. 5,711,147. Jan. 27, 1998. G.E. Vogtlin, B.T. Merritt, M.C. Hsiao, P.H. Wallman, B.M. Penetrante.

U.S. Patents Pending

NOx Reduction by Electron-Beam Produced Nitrogen Atom Injection.
DOE Patent Case No. S-93091, LLNL Invention Case No. IL-10572 (July 29, 1999). B.M. Penetrante.

Highly Basic Y Zeolite Catalysts for NOx Reduction at Low Temperatures.
DOE Patent Case No. S-93083, LLNL Invention Case No. IL-10564 (July 22, 1999). B.M. Penetrante, R.M. Brusasco, B.T. Merritt, G.E. Vogtlin.

Publications

Environmental Applications of Low-Temperature Plasmas.
Penetrante, B.M.; R.M. Brusasco, B.T. Merritt, W.J. Pitz, G.E. Vogtlin, *Pure and Applied Chemistry* **71**, 1829-1835 (1999).

Feasibility of Plasma Aftertreatment for Simultaneous Control of NO_x and Particulates.
Penetrante, B.M.; R.M. Brusasco, B.T. Merritt, W.J. Pitz, G.E. Vogtlin, SAE Paper Number 1999-01-3687, in Non-Thermal Plasma for Exhaust Emission Control: NOx, HC and Particulates (SAE/SP-99/1483, ISBN 0-7680-0490-X), (Society of Automotive Engineers, Warrendale, 1999) pp. 45-50.

Sulfur Tolerance of Selective Partial Oxidation of NO to NO_2 n a Plasma.
Penetrante, B.M.; R.M. Brusasco, B.T. Merritt, G.E. Vogtlin, SAE Paper Number 1999-01-3687, in Non-Thermal Plasma for Exhaust Emission Control: NOx, HC and Particulates (SAE/SP-99/1483, ISBN 0-7680-0490-X), (Society of Automotive Engineers, Warrendale, 1999) pp. 111-120.

Plasma-Assisted Catalytic Reduction of NO_x.
Penetrante, B.M.; R.M. Brusasco, B.T. Merritt, W.J. Pitz, G.E. Vogtlin, M.C. Kung, H.H. Kung, C.Z. Wan and K.E. Voss, SAE Paper Number 982508, in *Plasma Exhaust Aftertreatment* (SAE/SP-98/1395, ISBN 0-7680-0309-1), Edited by J. Hoard and H. Servati (Society of Automotive Engineers, Warrendale, 1998) pp. 57-66.

Exhaust Aftertreatment Using Plasma-Assisted Catalysis.

Penetrante,B.M., Clean Fuels 2000: The Race to Produce New Fuels and Engines, San Diego, CA (February 2000).

Hydrocarbon and Electrical Requirements in the Plasma During Treatment of NOx in Light-Duty Diesel Engine Exhaust.

Penetrante, B.M.; R.M. Brusasco, B.T. Merritt, W.J. Pitz, G.E. Vogtlin, Proceedings of1999 Diesel Engine Emissions Reduction Workshop, Castine, Maine (July 1999).

Feasibility of Plasma Aftertreatment for Simultaneous Control of NOx and Particulates.

Penetrante, B.M.; R.M. Brusasco, B.T. Merritt, W.J. Pitz, G.E. Vogtlin, Proceedings of 1999 Diesel Engine Emissions Reduction Workshop, Castine, Maine (July 1999).

Effect of Exhaust Temperature on NOx Reduction by Nitrogen Atom Injection.

Penetrante, B.M., Proceedings of 1999 Diesel Engine Emissions Reduction Workshop, Castine, Maine (July 1999).

Fate of SO_2 During Plasma Treatment of Diesel Engine Exhaust.

Penetrante, B.M.; R.M. Brusasco, B.T. Merritt, W.J. Pitz, G.E. Vogtlin, Proceedings of1999 Diesel Engine Emissions Reduction Workshop, Castine, Maine (July 1999).

NOx Conversion Chemistry in Plasma-Assisted Catalysis.

Penetrante, B.M.; R.M. Brusasco; B.T. Merritt; G.E. Vogtlin, Proceedings of the 1998 Diesel Engine Emissions Reduction Workshop, Castine, Maine (July 1998).